

# A Novel Verifiable Fingerprinting Scheme for Generative Adversarial Networks

Guanlin Li

Nanyang Technological University

guanlin001@e.ntu.edu.sg

Shangwei Guo

Chongqing University

gswei5555@gmail.com

Run Wang

Wuhan University

wangrun@whu.edu.cn

Guowen Xu

Nanyang Technological University

guowen.xu@ntu.edu.sg

Jiwei Li

Zhejiang University & Shannon.AI

jiwei\_li@shannonai.com

Han Qiu

Tsinghua University

qiuhan@tsinghua.edu.cn

Tianwei Zhang

Nanyang Technological University

tianwei.zhang@ntu.edu.sg

**Abstract**—This paper presents a novel fingerprinting scheme for the Intellectual Property (IP) protection of Generative Adversarial Networks (GANs). Prior solutions for classification models adopt adversarial examples as the fingerprints, which can raise stealthiness and robustness problems when they are applied to the GAN models. Our scheme constructs a composite deep learning model from the target GAN and a classifier. Then we generate stealthy fingerprint samples from this composite model, and register them to the classifier for effective ownership verification. This scheme inspires three concrete methodologies to practically protect the modern GAN models. Theoretical analysis proves that these methods can satisfy different security requirements necessary for IP protection. We also conduct extensive experiments to show that our solutions outperform existing strategies in terms of stealthiness, functionality-preserving and unremovability.

## I. INTRODUCTION

As a promising deep learning technology, Generative Adversarial Networks (GANs) [16] have been widely used in various applications, e.g., image and audio synthesis [12], [43], attribute editing [20], text-to-image translation [34]. Different from classification models which predict labels, GANs aim to produce new data samples following certain distributions or requirements. A GAN model is realized by a game between two neural network models: a generator tries to fabricate new samples indistinguishable from real samples, while a discriminator aims to identify the difference between them. Through this competition, the generator is spurred to produce high-quality data that meets users' demands.

Modern GAN models are designed to be more sophisticated to cope with complicated tasks and datasets. For instance, BigGAN [3] has 8.32 billion floating point operations (BFLOPs) while SAGAN [40] has 9.18 BFLOPs. The competition between the generator and discriminator in these models also becomes much fiercer and resource-hungry. Training such a production-level GAN model usually requires a large amount of computing resources, valuable data, and human expertise. Therefore, a well-trained GAN model (especially the generator) has become the core Intellectual Property (IP) of AI applications. It is important to protect such assets, and prevent illegitimate plagiarism, unauthorized distribution and reproduction of GAN models.

Generally speaking, existing copyright protection methods for deep learning models can be roughly divided into two categories. The first one is *watermarking*. The model owner embeds carefully-crafted watermarks into the target model by a parameter regularizer [41] or backdoor data poisoning [2], [26], [29], [52]. Later, the watermarks can be extracted from the model parameters or output as the ownership evidence. The second strategy is *fingerprinting*. The model owner generates unique sample-label pairs that can exclusively and exactly characterize the target model. Common approaches [4], [32] adopt adversarial examples to identify such fingerprint examples. Compared to watermarking, fingerprinting does not need to make modifications on the target model. Hence, it can better preserve the performance of the target model [4]. It also shows more applicability and convenience, especially for some scenarios where the model owner does not have the right or capability to modify the models obtained from a third party. Due to these advantages, fingerprinting is a more promising method for IP protection of deep learning models. This is what we will focus on in this paper.

The question we aim to answer is: *how can we fingerprint a given GAN model?* We look through existing works from two perspectives. First, we consider the solutions for fingerprinting classification models [4], [32]. Due to the inherent distinction between GAN and classification models, simply extending these methods to the GAN model can cause some effectiveness and security issues. Essentially, the output of a GAN model is a data sample with a much larger space than a label from a classification model. Hence, adversarial examples against GANs are more sensitive (i.e., less robust) to the changes in the model or input-output. It will be easier for an adversary to invalidate the fingerprints based on adversarial examples by slightly transforming the models or data samples. Besides, the adversarial output from a GAN model can be more anomalous than the adversarial label from a classification model, giving the model thief opportunities to detect the fingerprint and then manipulate the verification results. We conduct experiments to quantitatively demonstrate that the fingerprinting methods following those works are easier to remove or detect in the GAN scenario (Sections II and VII). It is necessary to design a fingerprinting scheme dedicated to GAN models.

Second, some methods were proposed to detect artificial media, attribute the sources and trace the legal responsibilities [48], [49], [50]. They achieved these goals by generating and recognizing fingerprinted images from GAN models. However, they may not be practical when applied to fingerprint GAN models for IP protection. For instance, some methods require the model owner to modify the target model with poisoned training set or special loss functions [49], [50], which violates our fingerprinting requirement. The fingerprinted images are not robust against model transformations, as model fine-tuning with different data samples can fool the model owner [48]. These methods will not be considered in this paper.

In this paper, we propose a novel fingerprinting scheme to protect the copyright of GAN models. The key innovation of our scheme is a *composite deep learning model* constructed from the target GAN model and a classifier. Specifically, to make the ownership verification stealthier, we aim to design a set of fingerprints, whose input samples and output samples from the target model are visually indistinguishable from normal ones. With this requirement, it seems impossible for the model owner to detect the plagiarism solely from the model response, as prior solutions require the output of the plagiarized model has large divergence from the ground truth. To address this issue, we propose to employ a classifier that can accurately identify the output from the plagiarized model, and assign unique labels to it.

The introduction of the classifier can provide stealthiness for the fingerprints. Besides, it can also enhance their effectiveness and robustness: although the model owner is not permitted to change the target model, he can freely modify the classifier to better recognize the fingerprint output even the adversary performs certain transformations over the target model or inference samples. This benefit cannot be achieved in prior solutions [4], [32].

We formally present our fingerprinting scheme, as well as the security requirements. Following this scheme, we provide three concrete designs and implementations that can be applied to practically protect GAN models. Specifically, in the first method (CFP-AE), the model owner can produce a set of fingerprint samples, whose output from the target model is adversarial examples exclusively for the owner’s classifier. In the second and third methods (CFP-iBDv1, CFP-iBDv2), the target model’s responses to the fingerprint samples are designed to be invisible backdoor samples [28], which can trigger the backdoor embedded in the classifier to produce unique labels. We leverage the Triplet Loss [38] and fine-grained categorization [11], [15] techniques to design novel loss functions, which can implant the backdoor into the classifier for better security and efficiency.

Theoretically, we prove that our fingerprinting scheme and three concrete designs satisfy the security requirements of *functionality-preserving*, *non-trivial ownership*, *unremovability* and *unforgeability*. Empirically, we evaluate our solutions with three state-of-the-art GAN models (AttGAN [20], StarGAN [9], STGAN [30]), and compare them with prior strategies. Experiments indicate that the fingerprints from our methods (especially CFP-iBDv2) can effectively distinguish target and non-target GAN models with higher confidence. Besides, they can maintain higher robustness against various model and image transformations.

## II. MOTIVATION AND DESIGN INSIGHT

### A. Background on Fingerprinting

Fingerprinting is a promising technique to protect the IP of deep learning models [4], [32]. Different from DNN watermarking [2], [52], the model owner constructs the fingerprint and conducts ownership verification without modifying the target model. This brings more convenience and applicability. Fig. 1a shows the scenario of model fingerprinting.

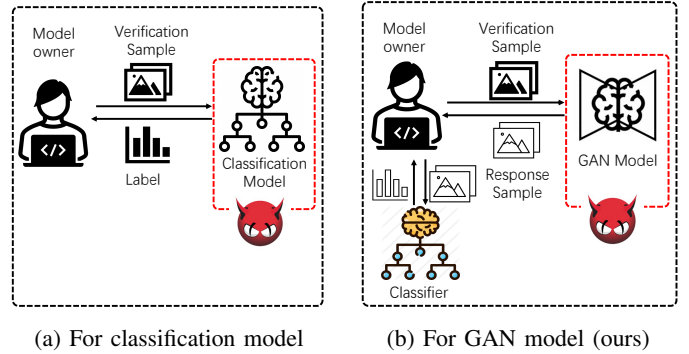


Fig. 1: Fingerprinting deep learning models.

**Threat model.** Given a protected deep learning model  $F$ , an adversary may obtain an illegal copy of  $F$  and use it for profit without authorization. The goal of the model owner is to detect whether a suspicious model  $F^s$  is plagiarized from  $F$ . The model owner has only oracle access to  $F^s$ , i.e., he can send arbitrary inputs to  $F^s$  and receive the corresponding outputs. The adversary may alter the inference process (e.g., model transformation or data sample modification) to perturb the verification results. However, such changes must be performed efficiently with limited computing resources, and maintain the usability of the model. The model owner needs to have a robust solution adaptive to those situations.

Researchers proposed solutions to fingerprint classification models leveraging the adversarial attacks [4], [32]. The key insight is to craft adversarial examples exclusively for the target model, which assigns unique labels to them. During verification, the model owner uses those samples to query a suspicious model. A matched model will give the desired unique labels, which serves as the evidence of ownership. An unrelated model will still predict normal ground-truth labels.

### B. Challenges to Fingerprint GAN Models

Existing works mainly focus on the classification models. It becomes difficult when we attempt to migrate these strategies to GANs. The main difference is that the output of a GAN is data samples rather than labels. Using adversarial examples of such models for fingerprinting can lead to two problems. First, the fingerprint is less *robust*: the output of GANs (e.g., images, audios) is more sensitive to model or input transformations than that of classifiers (labels). An adversary can easily remove the fingerprint from the protected model. We will present quantitative results for this conclusion in Section VII.

Second, the fingerprint is less *stealthy*: a unique label from a classification model is still reasonable, as it belongs

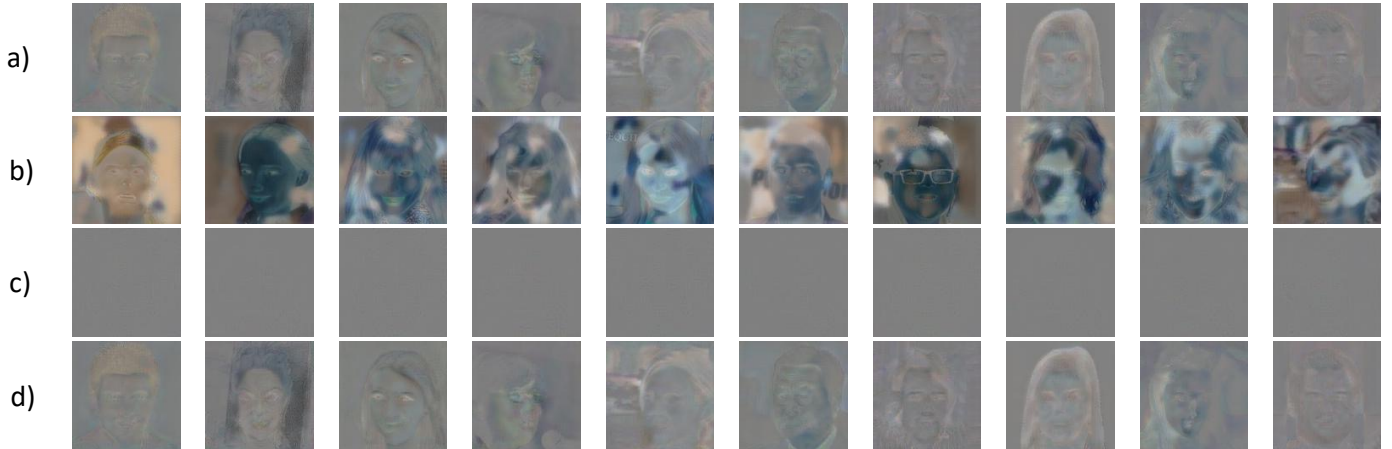


Fig. 2: Pixel differences between model output and input for different types of samples. (a) Clean samples. (b) Fingerprint samples based on  $l_2$ -norm AE-D. (c) Fingerprint samples based on  $l_2$ -norm AE-I. (d) Fingerprint samples based on our proposed scheme.

to one of possible classes. However, a unique data sample from a GAN can be suspicious, and easily recognized by the adversary, who will then manipulate the verification results. To demonstrate this, we consider a GAN (StarGAN [9]), which is capable of editing the facial attributes of the input images. We adopt the following two common adversarial attacks against GANs to generate fingerprints:

- AE-D: this is based on the *distortion attack* [14], [23], [36], [37], [47], where the outputs of the adversarial examples are distorted away from the correct ones. The adversary generates such perturbations by maximizing the distance between the adversarial output and original output.
- AE-I: this is based on the *identity attack* [37], [47], where the GAN model fails to make changes to the adversarial examples. This is achieved by minimizing the distance between the adversarial outputs and inputs.

We utilize the C&W technique [5] with the  $l_2$ ,  $l_1$  and  $l_\infty$ -norm to produce the above two types of adversarial samples. More implementation details can be found in Section VII. Fig. 2 shows the pixel differences of model outputs and inputs for various kinds of samples. Row (a) is the result of clean samples: the attributes of the person’s face are altered by the StarGAN model. Row (b) shows the fingerprint samples crafted from AE-D, where the difference is also distorted. The result of AE-I is displayed in Row (c), giving very small differences due to the identity attack. The distinct features of these fingerprint samples from clean ones make them easily recognizable. In contrast, Row (d) shows the result of our proposed scheme, which is very identical as the normal case.

An adversary can employ an anomaly detector to identify such anomalous fingerprint samples, and then refuse to respond, or return manipulated results. To show this feasibility, we train a one-class model based on the HRN approach [22], only from the clean samples. This model takes as input the inference samples and the corresponding results of the GAN model, and project them to a non-linear space  $(0, 1)$  through a function  $\text{sigmoid}(x) = 1/(1 + \exp^{-x})$ , where  $x$  is a feature representation from a backbone model (ResNet34 [18] in our implementation). The detection result of normal samples is expected to be close to 1, while that

of fingerprint samples is close to 0. We adopt a Negative Log Likelihood (NLL) loss function with a holistic regularization [22] to better classify the samples. More details about our anomaly detector can be found in Appendix A. Note that training such a detector is very efficient. The adversary can transfer a well-trained ResNet model to the one-class model with much smaller cost than training a state-of-the-art GAN model from the scratch. Besides, he can reuse this detector to guard other models for similar tasks. This motivates him to steal the GAN model and perform online detection.

Table 1 shows the performance of our anomaly detector. We adopt the AUC (Area Under the ROC Curve) metric, which considers both false

TABLE 1: AUC scores for detecting fingerprint samples.

Method	$l_2$	$l_1$	$l_\infty$
AE-D	85.74	99.82	86.39
AE-I	75.96	80.37	-
Ours	59.00	-	-

positives and false negatives. A higher AUC score means higher detection accuracy, while a score of 50 indicates the detector has similar performance as random guess. This table shows the anomaly detector can identify the fingerprint samples based on AE-D and AE-I<sup>1</sup> with high accuracy. A more stealthy fingerprinting scheme is desired to bypass the detector, as shown in the last row of the table (our solution).

### C. Design Insight

As discussed above, fingerprints for GANs based on adversarial examples might be recognized by the adversary. To make the verification stealthier and more indistinguishable from normal inference processes, *the fingerprint samples, the corresponding model output and inference behaviors should be identical to normal cases*. Besides, *the model output should also be unique to differentiate the target and other unrelated models*. These two conditions seem to contradict each other. We propose a new scheme to satisfy both of them. The general idea is that we craft fingerprint samples with the model output visually similar to normal ones, and employ a classifier to tell whether the output is from a target model or not (Fig. 1b).

<sup>1</sup>When generating samples with AE-I, we cannot find qualified samples bounded by the  $l_\infty$  norm.

A matched GAN model will produce visually normal output samples, which will be assigned unique labels by the classifier.

Note that the method in [48] also uses a classifier to detect GAN-generated images and attribute the sources. Different from that work, our scheme needs to carefully craft verification samples rather than normal ones, and modify the classifier accordingly to register the fingerprint. Hence, it exhibits better robustness against model transformations.

Below, we illustrate the formal definitions and abstract workflow of our proposed scheme in Section III, followed by the description of security requirements in Section IV. We provide three concrete methods based on our fingerprinting scheme in Section V. Sections VI and VII present the theoretical analysis and empirical evaluations about our methods.

### III. ABSTRACTION OF OUR FINGERPRINTING SCHEME

We focus on the copyright protection of a GAN without modifying the model. To achieve this, we introduce an additional classifier for ownership judgement, which forms a *composite deep learning model* with the target GAN. Then we carefully craft fingerprints and register them into the composite model. This process requires that the registered fingerprint should be difficult to remove even if the adversary modifies the model or samples.

Below, we give the formal definitions of the composite deep learning model and the fingerprint. Then, we review a widely-used cryptographic primitives called *commitments*, which is an important part of our protocol to be implemented credibly. Based on these, we give the workflow of our scheme. For simplicity, we use  $n \in \mathbb{N}$  as a security parameter, which is implicit in the input of all algorithms below. PPT indicates an algorithm that can be run in probabilistic polynomial time.  $[k]$  is the shorthand  $\{1, 2, \dots, k\}$  for  $k \in \mathbb{N}$ .

#### A. Composite Deep Learning Model

We consider a sample space  $D \subset \{0, 1\}^*$ , and a label space  $L \subset \{0, 1\}^* \cup \{\perp\}$  for any sample in  $D$ . We define  $|D| = \Theta(2^n)$  and  $|L| = \Omega(p(n))$  for a positive polynomial  $p(\cdot)$ . A composite deep learning model is defined as below:

**Definition 1.** (*Composite Deep Learning Model*) Let  $G$  be the target GAN model, which maps a sample  $x \in D$  to another sample  $x' \in D$ . Let  $f$  be a ground-truth function which classifies a sample  $x \in D$  according to its natural fixed label  $y \in L$ . Let  $\mathcal{G}(x) = \{G(x) \cup (G(x))^T | x \in D\}$ , where  $G(x)$  and  $(G(x))^T$  denote the accurate model outputs and perturbed ones by the adversary. Then a composite deep learning model is defined as  $M(x) = f'(\mathcal{G}(x))$ , where  $f'$  is the approximation of  $f$  through the **Train** algorithm described below.

The composite deep learning model is essentially a mapping  $M : D \rightarrow L$ , which simulates how humans assign specific labels to GAN-generated samples. To produce the composite model from  $G$  and  $f$ , we consider an oracle  $\mathcal{O}^f$ , which truly answers each call to  $f$ . Then we have the following algorithms.

- **Train**( $\mathcal{O}^f, G$ ): it is a probabilistic polynomial time algorithm used to output a model  $M \subset \{0, 1\}^{p(n)}$ , where  $p(n)$  is a polynomial in  $n$ .

- **Classify**( $M, x$ ): it is a deterministic function that outputs a value  $M(x) \in L \setminus \{\perp\}$  for a given input  $x \in D$ .

We use  $\bar{D} = \{x \in D | M(x) \neq \perp\}$  to denote the set of all inputs whose relationship with the output is defined. Then we say the algorithms (**Train**, **Classify**) are  $\epsilon$ -accurate if  $Pr[f(\mathcal{G}(x)) \neq \text{Classify}(M, x) | x \in \bar{D}] \leq \epsilon$ , where the probability arises from the randomness of **Train**. Thus, we measure accuracy mainly for those inputs that are meaningful to the outputs. For those inputs not defined by the ground-truth classifier  $f$ , we assume their labels are random, i.e., for all  $x \in D \setminus \bar{D}$  and any  $i \in L$ , we have  $Pr[\text{Classify}(M, x) = i] = 1/|L|$ .

#### B. Fingerprints in Composite Deep Learning Models

Our fingerprinting scheme crafts a set of verification samples and a classifier, such that the classifier can assign unique labels to the target model's outputs of these verification samples. Formally, we have the following definition:

**Definition 2.** (*Fingerprint Set for a Composite Model*) A *fingerprint set*  $\mathcal{V}$  for a composite model  $M$  is defined as  $(V, V_L)$ , where the verification sample set  $V \subset D$  and verification label set  $V_L \subset L \setminus \{\perp\}$  satisfy the condition: for  $x \in V$ ,  $V_L(x) \neq f(\mathcal{G}(x))$ .

We use an algorithm  $\mathbf{F}_{\text{gen}}$  to generate a fingerprint set<sup>2</sup> from the target GAN model  $G$  and oracle  $\mathcal{O}^f$ . We further define a PPT algorithm called  $\mathbf{F}_{\text{reg}}$  to register the generated fingerprint into the composite model. Specifically, given the oracle  $\mathcal{O}^f$ , a fingerprint set  $\mathcal{V}$ , and a composite model  $M$ ,  $\mathbf{F}_{\text{reg}}$  produces a fingerprinted model  $\hat{M} = \hat{f}(\mathcal{G}(\cdot))$ , which can correctly classify the verification samples  $V$  as  $V_L$  with a high probability. Formally, we have the following definition:

**Definition 3.** (*Fingerprinted Model*) We say a composite model  $M$  is fingerprinted by  $\mathbf{F}_{\text{reg}}$ , if it behaves like  $f(\mathcal{G}(\cdot))$  on  $\bar{D} \setminus V$ , and reliably predict unique labels  $V_L$  on  $V$ , i.e.,

$$\begin{aligned} Pr_{x \in \bar{D} \setminus V} [f(\mathcal{G}(x)) \neq \text{Classify}(\hat{M}, x)] &\leq \epsilon, \text{ and} \\ Pr_{x \in V} [V_L(x) \neq \text{Classify}(\hat{M}, x)] &\leq \epsilon. \end{aligned} \quad (1)$$

*Remark:* since a given model may be suspected of being registered in fingerprints, a strong fingerprint should be difficult to be reconstructed or detected by adversaries in arbitrary ways. It requires the fingerprints to satisfy additional requirements to endure various types of attacks. For legibility, we leave the presentation of these requirements in Section IV.

#### C. Commitments

We adopt the commitment scheme to implement our verification protocol. Commitment [24] is a widely used cryptographic primitive that allows the sender to lock a secret  $x$  in a vault that is free of cryptographic information leakage and tamper-proof, and then send it to someone else (i.e., a receiver). Generally, a commitment scheme contains two algorithms:

- **Com**( $x, h$ ): Given a secret  $x \in S$  and a random bit string  $h \in \{0, 1\}^n$ , outputs a bit string  $c_x$ .

<sup>2</sup>Whenever we fix a verification sample set  $V$ , the fingerprint set implies the corresponding  $V_L$ .

- **Open**( $c_x, x, h$ ): Given a secret  $x \in S$ , a random bit string  $h \in \{0, 1\}^n$ , and a  $c_x \in \{0, 1\}^*$ , outputs 0 or 1.

A commitment scheme enjoys the following properties:

**Correctness:** it is required that for  $\forall x \in S$ , we have

$$\Pr_{h \in \{0,1\}^n} [\mathbf{Open}(c_x, x, h) = 1 | \mathbf{Com}(x, h) \rightarrow c_x] = 1$$

**Hiding:** it is infeasible for receivers to open the locked  $x$  without the sender's help. For any PPT algorithm  $\mathcal{A}$ , we have

$$\Pr \left[ \mathbf{Open}(c_x, \tilde{x}, \tilde{h}) = 1 \mid \begin{array}{l} c_x \leftarrow \mathbf{Com}(x, h) \wedge \\ (\tilde{x}, \tilde{h}) \leftarrow \mathcal{A}(c_x, x, h) \wedge \\ (x, h) \neq (\tilde{x}, \tilde{h}) \end{array} \right] \leq \epsilon(n)$$

where  $\epsilon(n)$  is negligible in  $n$  and the probability is taken over  $x \in S$  and  $h \in \{0, 1\}^n$ .

**Biding:** it is impossible for the sender to change the locked secret  $x$  once it is sent out. It requires that no PPT algorithm  $\mathcal{A}$  can distinguish  $c_0 \leftarrow \mathbf{Com}(0, h)$  from  $c_x \leftarrow \mathbf{Com}(x, h)$  for any  $x \in S$  and  $h \in \{0, 1\}^n$ . If the distributions of  $c_0$  and  $c_x$  are statistically close, we call the commitment scheme statistical hiding. For more details, please refer to [2], [24].

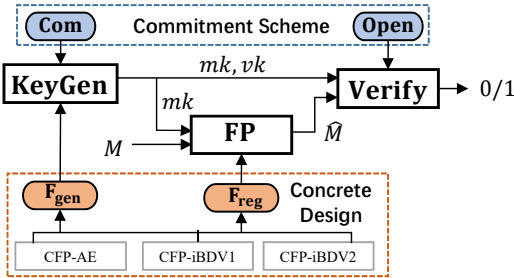


Fig. 3: The workflow of our fingerprinting scheme.

#### D. Workflow of Our Fingerprinting Scheme

We now outline the fingerprinting process for a general composite deep learning model. As shown in Fig. 3, a model owner essentially uses a series of algorithms to generate a secret marking key  $mk$  and a public verification key  $vk$ , and register the fingerprint from  $mk$  into the model. During verification, the model owner uses marking and verification keys to verify whether a suspicious model contains the fingerprints. To be more precise, the entire workflow can be described by three high-level PPT algorithm (**KeyGen**, **FP**, **Verify**):

- **KeyGen**( $n, M$ ): Given the security parameter  $n$  and the information related to the model, it outputs the secret marking key  $mk$  and the public verification key  $vk$ , where  $mk$  contains the fingerprint for registering into the target model, and  $vk$  is used for subsequent verification. This process requires  $\mathbf{F}_{\text{gen}}$  to generate fingerprint sets. It also requires **Com** to commit to the elements in each fingerprint set and random elements selected by model owner, which provides arguments for subsequent verification.
- **FP**( $M, mk$ ): Given a composite model  $M$  and the marking key  $mk$ , it outputs a fingerprinted model  $\hat{M}$ . This process uses  $\mathbf{F}_{\text{reg}}$  as the subroutine to convert  $M$  to  $\hat{M}$ , thereby registering the selected fingerprint contained in  $mk$  into  $M$ .
- **Verify**( $mk, vk, \hat{M}$ ): Given the key pair  $mk, vk$  and a model  $\hat{M}$ , it outputs a bit  $b \in \{0, 1\}$ , where 1 means

that the verified model has copyright infringement, and vice versa. This process uses **Open** as the subroutine to open the previous commitments to all the elements in  $mk$ .

We will provide comprehensive technical details in Section V, including how to generate qualified fingerprints, registering models, and copyright verification.

## IV. SECURITY REQUIREMENTS FOR FINGERPRINTING

We first define the concept of strong fingerprint and its properties. Then we introduce the security requirements that a qualified fingerprinting scheme should satisfy.

### A. Strong Fingerprint

With the two algorithms  $\mathbf{F}_{\text{gen}}$  and  $\mathbf{F}_{\text{reg}}$ , we expect that the model owner is able to produce strong fingerprints  $\mathcal{V}$  that can satisfy the following three properties. As a result,  $\mathbf{F}_{\text{reg}}$  that takes such samples as input is called a strong fingerprinting algorithm. These are necessary for us to build effective fingerprinting solutions.

(1) *Multiple verification sample sets:* We assume that  $\mathbf{F}_{\text{gen}}$  can output a fingerprint set of size  $n$  each time. To generate strong fingerprints,  $\mathbf{F}_{\text{gen}}$  is required to execute iteratively. Moreover, for two random fingerprint sets generated by  $\mathbf{F}_{\text{gen}}$  from the same composite model, we require their verification sample sets  $V$  and  $V'$  almost never intersect, i.e.,  $\Pr[V \cap V'] \neq \emptyset$  for  $(V, V_L), (V', V'_L) \leftarrow \mathbf{F}_{\text{gen}}()$  is negligible in  $n$ .

(2) *Stealthiness:* Each verification sample and inference process should be indistinguishable from the normal ones, making it difficult for the adversary to respond adaptively and ensuring the concealment of verification. This means that for each verification sample  $v^{(i)} \in V$  generated from a randomly selected clean sample  $x^{(i)}$ , the following expression:

$$\mathcal{H} = \|v^{(i)}, x^{(i)}\| + \|G(v^{(i)}), G(x^{(i)})\| + \sum_j \|G_{v^{(i)}, j}, G_{x^{(i)}, j}\|$$

is minimized, where  $G_{v^{(i)}, j}$  and  $G_{x^{(i)}, j}$  are the  $j$ -th feature maps in  $G$ , and  $\|\cdot, \cdot\|$  is a distance function.

Note that the stealthiness of fingerprints is difficult to describe with cryptographic primitives, because it is very subjective and varies from person to person. In this paper, we mainly demonstrate the superiority of the generated fingerprint based on empirical experiments (Section VII-B).

(3) *Persistence:*  $\mathbf{F}_{\text{reg}}$  is able to register the fingerprint persistently such that the adversary cannot revert the fingerprinted model back to the original one. This property is discussed under two assumptions. First, the adversary has limited computing resources, which do not support him to retrain a clean model from scratch. Otherwise, he will lose the motivation of stealing others' models. Second, the adversary is not willing to erase the fingerprint at the cost of huge accuracy drop for the plagiarized model. Hence, given the oracle  $\mathcal{O}^f$ , a fingerprint set  $\mathcal{V}$ , and  $\hat{M} \leftarrow \mathbf{F}_{\text{reg}}(\mathcal{O}^f, \mathcal{V}, M)$ , we define the persistence as follows: assume an algorithm  $\mathcal{A}$  on input  $\mathcal{O}^f, \hat{M}$  outputs a model  $\tilde{M}$  with  $\epsilon$ -accurate in polynomial time  $t$ , where  $\tilde{M}$  is at least  $(1 - \epsilon)$  accurate on  $\mathcal{V}$ . Further, for any arbitrary model  $N, \tilde{N} \leftarrow \mathbf{F}_{\text{reg}}(\mathcal{O}^f, N)$  generated in time  $t$ , is also  $\epsilon$ -accurate.

## B. Security Requirements for Fingerprinting Schemes

A fingerprinting scheme consists of three PPT algorithms (**KeyGen**, **FP**, **Verify**). Their correctness requires that for the honestly generated keys  $mk, vk$ , we have

$$\Pr_{(M, \hat{M}, mk, vk)} [\mathbf{Verify}(mk, vk, \hat{M}) = 1] = 1.$$

We now define the following four security requirements for a qualified fingerprinting scheme:

(I) **Functionality-preserving.** We say that a fingerprinting scheme is functionality preserving, if the model with fingerprints is as accurate as the model without fingerprints. Formally, for any  $(M, \hat{M}, mk, vk)$  honestly generated through the previously described algorithms, it holds that

$$\begin{aligned} & \Pr_{x \in \bar{D}} [\mathbf{Classify}(M, x) = f(\mathcal{G}(x))] \\ & \approx \Pr_{x \in \bar{D}} [\mathbf{Classify}(\hat{M}, x) = f(\mathcal{G}(x))]. \end{aligned}$$

(II) **Non-trivial ownership.** This property requires that it is impossible for an adversary to construct a key pair  $(mk, vk)$  in advance to claim the ownership of an arbitrary model that is unknown to him, even if he knows the fingerprinting algorithm. Formally, a fingerprinting scheme with non-trivial ownership requires that any PPT algorithm  $\mathcal{A}$  wins the following game only with a negligible probability.

### Game 1:

1. Run  $\mathcal{A}$  to compute  $(\tilde{mk}, \tilde{vk}) \leftarrow \mathcal{A}()$ .
2. Generate  $M \leftarrow \mathbf{Train}(\mathcal{O}^f, G)$ .
3. Sample  $(mk, vk) \leftarrow \mathbf{KeyGen}()$ .
4. Compute  $\hat{M} \leftarrow \mathbf{FP}(M, mk)$ .
5.  $\mathcal{A}$  wins if  $\mathbf{Verify}(mk, \tilde{vk}, \hat{M})=1$ .

(III) **Unremovability.** This means that the adversary cannot remove the fingerprint even if he knows its existence and the algorithms used in the process. Formally, a fingerprinting scheme with unremovability requires that any PPT algorithm  $\mathcal{A}$  wins the following game only with a negligible probability.

### Game 2:

1. Generate  $M \leftarrow \mathbf{Train}(\mathcal{O}^f, G)$ .
2. Sample  $(mk, vk) \leftarrow \mathbf{KeyGen}()$ .
3. Compute  $\hat{M} \leftarrow \mathbf{FP}(M, mk)$ .
4. Run  $\mathcal{A}$  to compute  $\tilde{M} \leftarrow \mathcal{A}(\mathcal{O}^f, \hat{M}, vk)$ .
5.  $\mathcal{A}$  wins if

$$\begin{aligned} & \Pr_{x \in D} [\mathbf{Classify}(M, x) = f(\mathcal{G}(x))] \\ & \approx \Pr_{x \in D} [\mathbf{Classify}(\tilde{M}, x) = f(\mathcal{G}(x))] \\ & \text{and } \mathbf{Verify}(mk, vk, \tilde{M}) = 0. \end{aligned}$$

(IV) **Unforgeability.** This property requires that even if the adversary knows  $vk$ , he cannot convince a third party that he has the property rights to the model without knowing  $mk$ . Formally, a fingerprinting scheme with unforgeability requires that any PPT algorithm  $\mathcal{A}$  wins the following game only with negligible probability.

### Game 3:

1. Generate  $M \leftarrow \mathbf{Train}(\mathcal{O}^f, G)$ .
2. Sample  $(mk, vk) \leftarrow \mathbf{KeyGen}()$ .
3. Compute  $\hat{M} \leftarrow \mathbf{FP}(M, mk)$ .
4. Run the adversary  $(\tilde{mk}, \tilde{M}) \leftarrow \mathcal{A}(\mathcal{O}^f, \hat{M}, vk)$ .
5.  $\mathcal{A}$  wins if  $\mathbf{Verify}(\tilde{mk}, vk, \tilde{M})=1$ .

## V. CONCRETE FINGERPRINTING CONSTRUCTION

We present some novel concrete designs based on our fingerprinting scheme. For each design, we describe the two crucial algorithms  $\mathbf{F}_{\text{gen}}$  and  $\mathbf{F}_{\text{reg}}$  for generating strong fingerprints and registering them into the model, respectively.

### A. CFP-AE

Our first fingerprinting method, CFP-AE (Composite Fingerprint based on Adversarial Examples), is inspired by the generative adversarial examples [44]. Different from the traditional fingerprinting methods [4], [32] that directly craft adversarial examples against the target model, we propose to make the target GAN model generate adversarial examples against the classifier. The output sample of the target GAN model looks normal, while the output label of the classifier is unique as the ownership evidence.

Algorithm 1 shows the detailed process of generating the fingerprint set. We first train a ground-truth classifier  $f$  for classifying the attributes of the data samples. Then we uniformly select some random samples  $x^{(i)}$  from the sample space  $D$ . Since the size of the space is  $\Theta(2^n)$ , a PPT adversary only has a negligible probability to infer these samples. We craft the verification samples  $v^{(i)}$  from these clean samples using an optimization method. To ensure the indistinguishability between the verification sample and its corresponding clean sample, we need to minimize  $\mathcal{H} = \|v^{(i)}, x^{(i)}\| + \|G(v^{(i)}), G(x^{(i)})\| + \sum_j \|G_{v^{(i)}, j}, G_{x^{(i)}, j}\|$ . To make the classifier give unique labels, we need to maximize the distance between the normal label  $y^{(i)}$  and predicted label  $f(G(v^{(i)}))$ . We construct a loss function  $F_{\text{obj}}(\mathcal{O}^f, G, \{x^{(i)}, y^{(i)}\}, v^{(i)})$  to satisfy these goals:

$$\begin{aligned} F_{\text{obj}}(\mathcal{O}^f, G, \{x^{(i)}, y^{(i)}\}, v^{(i)}) &= - \sum_c y_c^{(i)} \log(f(G(v^{(i)}))_c) \\ &+ \sum (v^{(i)} - x^{(i)})^2 + \sum (G(v^{(i)}) - G(x^{(i)}))^2 \\ &+ \sum_j \sum (G_{v^{(i)}, j} - G_{x^{(i)}, j})^2, \end{aligned} \quad (2)$$

where  $G_{v^{(i)}, j}$  and  $G_{x^{(i)}, j}$  are the  $j$ -th feature maps in  $G$  when processing  $v^{(i)}$  and  $x^{(i)}$ , respectively. We iteratively search for the optimal  $v^{(i)}$  by minimizing the above objective function, and obtain the final verification sample  $v^{(i)}$ , and verification label  $v_L^{(i)} = f(G(v^{(i)}))$ .

---

### Algorithm 1: Fingerprint Generation

---

$\mathbf{F}_{\text{gen}}(\mathcal{O}^f, G)$

- 1: Uniformly select random samples  $\{x, y\} \in \bar{D}$   $n$  times to build  $X = \{x^{(1)}, \dots, x^{(n)}\}$  and  $Y = \{y^{(1)}, \dots, y^{(n)}\}$ .
  - 2: **for each**  $\{x^{(i)}, y^{(i)}\} \in \{X, Y\}$  **do**
  - 3:   Generate  $v^{(i)}$  from  $\{x^{(i)}, y^{(i)}\}$  by minimizing the objective function  $F_{\text{obj}}(\mathcal{O}^f, G, \{x^{(i)}, y^{(i)}\}, v^{(i)})$  in Equation 2.
  - 4:    $v_L^{(i)} = f(G(v^{(i)}))$
  - 5: **end for**
  - 6: **Return** a fingerprint  $\mathcal{V} = (V, V_L)$ , where  $V = \{v^{(1)}, \dots, v^{(n)}\}$  and  $V_L = \{v_L^{(1)}, \dots, v_L^{(n)}\}$ .
- 

It is worth noting that in CFP-AE, we do not need to modify the classifier  $f$  after we perform the  $\mathbf{F}_{\text{gen}}$  function. We can directly use the generated samples to query the composite model for ownership verification. Hence, the  $\mathbf{F}_{\text{reg}}$  function is empty with  $\hat{f} = f$  in this method.

## B. CFP-iBDv1

Our second method, CFP-iBDv1 (Composite Fingerprint based on invisible Backdoor (version 1)), utilizes the invisible backdoor attack technique [28]. The key idea is to make the target model produce output samples containing invisible triggers, which will activate the backdoor embedded in the classifier to predict unique labels. CFP-iBDv1 requires two steps. Fingerprint generation calls the same function  $\mathbf{F}_{\text{gen}}$  as in CFP-AE to produce a set of verification samples and labels. Then we perform the fingerprint registering  $\mathbf{F}_{\text{reg}}(\mathcal{O}^f, \mathcal{V}, M)$ , which fine-tunes the classifier  $f$ , to better recognize the relationships between the verification samples and labels.

Algorithm 2 shows the detailed process of fine-tuning the classifier. We prepare two sets: the verification set  $\mathcal{V}_s = (G(V), V_L)$  is generated from  $\mathbf{F}_{\text{gen}}$ ; the normal set  $\mathcal{N}_s = (G(X), M(X))$  is sampled from the data space  $X \in \bar{D} \setminus V$ . Since the fingerprint must be persistent against image transformations, we further perform data augmentation over these two sets with common transformation functions. Using these two augmented sets  $\mathcal{V}_s^a$  and  $\mathcal{N}_s^a$ , we fine-tune the classifier as  $\hat{f}$ , and finally obtain the composite model  $\hat{M}(\cdot) = \hat{f}(\mathcal{G}(\cdot))$ .

---

### Algorithm 2: Fingerprint Registering

---

- $\mathbf{F}_{\text{reg}}(\mathcal{O}^f, \mathcal{V}, M)$
- 1:  $(V, V_L) = \mathbf{F}_{\text{gen}}(\mathcal{O}^f, G)$ .
  - 2: Sample  $X$  from  $\bar{D} \setminus V$  and compute the label  $M(X)$ .
  - 3:  $\mathcal{V}_s = (G(V), V_L)$ .
  - 4:  $\mathcal{N}_s = (G(X), M(X))$ .
  - 5: Augment these two sets to obtain  $\mathcal{V}_s^a$  and  $\mathcal{N}_s^a$ .
  - 6: Fine-tune  $f$  into  $\hat{f}$  with  $\mathcal{V}_s^a$  and  $\mathcal{N}_s^a$  together by minimizing the loss function  $\mathcal{L}_{ft}$ .
  - 7: **Return** fingerprinted model  $\hat{M}(\cdot) = \hat{f}(\mathcal{G}(\cdot))$ .
- 

We use the cross-entropy loss function to fine-tune the classifier with the two sets:

$$\mathcal{L}_{ft} = \mathcal{L}_{G1}(f, \mathcal{V}_s^a, \mathcal{N}_s^a) = - \sum_{(x,y) \in \mathcal{V}_s^a} \sum_c y_c \log(f(x)_c) - \sum_{(x,y) \in \mathcal{N}_s^a} \sum_c y_c \log(f(x)_c),$$

where  $c$  is the label index of  $f$ .

## C. CFP-iBDv2

Our third method, CFP-iBDv2 (Composite Fingerprint based on invisible Backdoor (version 2)), is an advanced version of CFP-iBDv1. We follow the same algorithms to generate fingerprints and register them into the model. A novel loss function is introduced to fine-tune the classifier for better robustness and effectiveness.

First, we adopt the idea of the Triplet Loss [38] to enhance the persistency of our fingerprints. The Triplet Loss is able to distinguish different objects under similar conditions (e.g., pose, illumination). It achieves this by minimizing the inner representation (i.e., feature embedding) difference of the same object with different external conditions, while maximizing the difference of different objects with the same condition. Similarly, we can minimize the distance of different verification samples in the feature space, and maximize the distance of a verification and normal samples. This can increase the

probability that the fine-tuned classifier will give unique labels for verification samples. The loss function is as below:

$$\mathcal{L}_{G2}(\mathcal{M}, \mathcal{V}_s^a, \mathcal{N}_s^a, m) = \sum_{v_a \in \mathcal{V}_s^a} \max_{v_p \in \mathcal{V}_s^a} \left\{ \max_{v_p \in \mathcal{V}_s^a} \left( \sum (\mathcal{M}(v_a) - \mathcal{M}(v_p))^2 \right) - \min_{x \in \mathcal{N}_s^a} \left( \sum (\mathcal{M}(v_a) - \mathcal{M}(x))^2 \right) + m, 0 \right\},$$

where  $m$  is a constant, and  $\mathcal{M}(\cdot)$  represents the feature embedding in the feature space before the classification layers.

Second, we apply the fine-grained categorization approaches [11], [15] to fine-tune the classifier. Fine-grained categorization aims to classify an object into an exact sub-category, e.g., the brand of a car, the species of a bird. Various techniques have been introduced to achieve this challenging goal [33], [46], [51]. We can treat the fingerprint registration process as a fine-grained categorization task, where samples from  $\mathcal{V}_s^a$  are in one category (fingerprint verification), while samples from  $\mathcal{N}_s^a$  are in another category (normal inference). Specifically, we change the classifier to a multitask one: the original network is used to predict the attribute, while a new classification layer is added to predict the verification category (label “1” for fingerprint verification; label “0” for normal inference). Then we adopt the Entropy-Confusion Loss [13] to train the multi-task model:

$$\mathcal{L}_{G3}(\mathcal{B}, \mathcal{V}_s^a, \mathcal{N}_s^a, \epsilon) = \sum_{v \in \mathcal{V}_s^a} (\mathcal{B}(v)_0 \log \frac{\mathcal{B}(v)_0}{\epsilon} + (\mathcal{B}(v)_1 + 1) \log \mathcal{B}(v)_1) + \sum_{x \in \mathcal{N}_s^a} ((\mathcal{B}(x)_0 + 1) \log \mathcal{B}(x)_0 + \mathcal{B}(x)_1 \log \frac{\mathcal{B}(x)_1}{\epsilon}),$$

where  $\epsilon = 1e^{-5}$  is a constant to avoid a denominator of zero,  $\mathcal{B}(\cdot)$  is the output from the added binary classification layer, and  $\mathcal{B}(\cdot)_i$  is the  $i$ -th element in the output. Hence, our ultimate loss function  $\mathcal{L}_{ft}$  used to fine-tune  $f$  is

$$\mathcal{L}_{ft} = \mathcal{L}_{G1} + \mathcal{L}_{G2} + \mathcal{L}_{G3}.$$

After we finish the classifier fine-tuning, we remove the binary classification layer from  $\hat{f}$ , and integrate it with the target GAN model to form the composite model  $\hat{M}$ .

	Concrete Construction
<b>KeyGen():</b>	<ol style="list-style-type: none"> <li>1. Run <math>(V, V_L) = \mathcal{V} \leftarrow \mathbf{F}_{\text{gen}}(\mathcal{O}^f, G)</math>, where <math>V = \{v^{(1)}, \dots, v^{(n)}\}</math> and <math>V_L = \{v_L^{(1)}, \dots, v_L^{(n)}\}</math>.</li> <li>2. Sample <math>2n</math> random strings <math>h_v^{(i)}, h_L^{(i)} \leftarrow \{0, 1\}^n</math>, generate <math>2n</math> commitments <math>\{c_v^{(i)}, c_L^{(i)}\}_{i \in [n]}</math>, where <math>c_v^{(i)} \leftarrow \mathbf{Com}(v^{(i)}, h_v^{(i)})</math>, <math>c_L^{(i)} \leftarrow \mathbf{Com}(v_L^{(i)}, h_L^{(i)})</math>.</li> <li>3. Set <math>mk \leftarrow (\mathcal{V}, \{h_v^{(i)}, h_L^{(i)}\}_{i \in [n]})</math>, <math>vk \leftarrow \{c_v^{(i)}, c_L^{(i)}\}_{i \in [n]}</math> and return <math>(mk, vk)</math>.</li> </ol>
<b>FP(<math>M, mk</math>):</b>	<ol style="list-style-type: none"> <li>1. Let <math>mk = (\mathcal{V}, \{h_v^{(i)}, h_L^{(i)}\}_{i \in [n]})</math>.</li> <li>2. Compute and output <math>\hat{M} \leftarrow \mathbf{F}_{\text{reg}}(\mathcal{O}^f, \mathcal{V}, M)</math>.</li> </ol>
<b>Verify(<math>mk, vk, M</math>):</b>	<ol style="list-style-type: none"> <li>1. Let <math>mk \leftarrow (\mathcal{V}, \{h_v^{(i)}, h_L^{(i)}\}_{i \in [n]})</math>, <math>vk \leftarrow \{c_v^{(i)}, c_L^{(i)}\}_{i \in [n]}</math>. For <math>\mathcal{V} = (V, V_L)</math>, test if <math>\forall v^{(i)} \in V</math>: <math>v_L^{(i)} \neq f(\mathcal{G}(v^{(i)}))</math>. If not, then output 0.</li> <li>2. Check that <math>\mathbf{Open}(c_v^{(i)}, v^{(i)}, h_v^{(i)}) = 1</math> and <math>\mathbf{Open}(c_L^{(i)}, v_L^{(i)}, h_L^{(i)}) = 1</math> for all <math>i \in [n]</math>. Otherwise, output 0.</li> <li>3. Test that <math>\mathbf{Classify}(M, v^{(i)}) = v_L^{(i)}</math> for all <math>i \in [n]</math>. If this is true for all except <math>\epsilon \mathcal{V} </math> elements from <math>\mathcal{V}</math>, then output 1, otherwise output 0.</li> </ol>

Fig. 4: Concrete construction of a fingerprinting process.

#### D. Concrete Construction

With  $\mathbf{F}_{\text{gen}}$  and  $\mathbf{F}_{\text{reg}}$  from either one of the above three methods, we can construct an end-to-end process for model fingerprinting. Fig. 4 shows the high-level algorithms (**KeyGen**, **FP**, **Verify**) for this process. Specifically, let (**Train**, **Classify**) be an  $\epsilon$ -accurate composite deep learning model,  $\mathbf{F}_{\text{reg}}$  be a strong fingerprinting algorithm and (**Com**, **Open**) be a statistically hiding commitment scheme. (1) **KeyGen** generates strong fingerprints ( $\mathbf{F}_{\text{gen}}$ ), which are also used as the secret marking key  $mk$ . Then a commitment scheme (**Com**) is used to generate the verification key  $vk$  corresponding to  $mk$  for the legitimacy verification of suspicious models. (2) **FP** registers the fingerprints into the composite model ( $\mathbf{F}_{\text{reg}}$ ). (3) **Verify** opens the commitments (**Open**) to all the elements in the secret key  $mk$ , and uses it to verify whether a suspicious model matches the fingerprints (**Classify**). If most verification samples in the fingerprint set are predicted as the verification labels by the classifier  $\hat{f}$ , we infer that this GAN model is infringing.

### VI. SECURITY ANALYSIS

We now prove the security of the above construction. Specifically, we give the following theorem:

**Theorem 1.** *Let  $\bar{D}$  be of super-polynomial size in  $n$ . Given the commitment scheme and the strong fingerprinting algorithm, the above algorithms (**KeyGen**, **FP**, **Verify**) form a privately verifiable fingerprinting scheme, which satisfies the requirements of functionality-preserving, non-trivial ownership, unremovability, and unforgeability.*

*Proof:* As defined in Section IV, a strong fingerprint registered into the model cannot be removed by the adversary in time  $t$ . In addition, the *hiding* property of the commitment scheme enables the public verification key to hide useful information about the fingerprint from the adversary, while the *binding* property ensures that one cannot claim the ownership of a model from others. Based on these, we prove the satisfaction of the following requirements:

(I) **Functionality-preserving.** By the definition of the algorithm  $\mathbf{F}_{\text{reg}}$ , it outputs a model  $\hat{M}$  that satisfies

$$\Pr_{x \in \bar{D} \setminus V} [f(\mathcal{G}(x)) \neq \mathbf{Classify}(\hat{M}, x)] \leq \epsilon, \text{ and}$$

$$\Pr_{x \in V} [V_L(x) \neq \mathbf{Classify}(\hat{M}, x)] \leq \epsilon.$$

As a result, given the error  $\epsilon$ ,  $\hat{M}$  classifies correctly for at least  $(1 - \epsilon)|\mathcal{V}|$  elements in  $\mathcal{V}$ , which is consistent with the argument that **Classify** outputs 1 if  $\hat{M}$  disagrees with  $\mathcal{V}$  on at most  $\epsilon|\mathcal{V}|$  elements.

(II) **Non-trivial ownership.** As defined in **Game 1**, if  $\mathcal{A}$  wants to win, he must guess the correct labels for a  $(1 - \epsilon)$  fraction of  $\tilde{V}$  in advance, since he cannot change the selected  $\tilde{V}$  and  $\tilde{V}_L$  after seeing the model. This is determined by the binding property of the commitment scheme. On the other hand, since the algorithm **KeyGen** generates the set  $V$  in  $mk$  in a uniformly random space,  $mk$  fixed by any algorithm  $\mathcal{A}$  has a negligible probability of intersection with  $V$  (due to the property of *multiple verification sample sets*). For simplicity, we assume that  $\tilde{V}$  and  $V$  will not intersect with each other.

Now  $\mathcal{A}$  can generate  $\tilde{V}$  either from space in  $\bar{D}$  or outside of  $D$ . Let  $n_1 = |\bar{D} \cap \tilde{V}|$  and  $n_2 = |\tilde{V}| - n_1$ .

For the benefit of the adversary, we give a strong assumption that whenever  $M$  misclassifies the input  $x \in \bar{D} \cap \tilde{V}$ , the label of  $x$  is in  $\tilde{V}_L$ . However, since  $M$  is  $\epsilon$ -accurate on  $\bar{D}$ , the ratio of incorrectly classified committed label is  $(1 - \epsilon)$ . We have  $\epsilon n_1 < (1 - \epsilon)n_1$  for every choice  $\epsilon < 0.5$ . Because in our scheme,  $\epsilon$  is usually much smaller than 0.5, the above inequality always holds. On the other hand, if all the values in  $\tilde{V}$  fall in  $D \setminus \bar{D}$ , according to the definition of the composite deep learning model,  $M$  will misclassify  $\frac{L-1}{|L|}n_2$  elements in expectation. We have  $\epsilon n_2 < \frac{L-1}{|L|}n_2$  as  $\epsilon < 0.5$  and  $L \geq 2$ . Since  $\epsilon n = \epsilon n_1 + \epsilon n_2$ , the error of  $\tilde{V}$  must be larger than  $\epsilon n$ .

(III) **Unremovability.** As defined in Section IV-A, we assume that no algorithms can generate an  $\epsilon$ -accurate model  $N$  in the time  $t$  of  $f$ , where  $t$  is much smaller than the time required to train a model with the same accuracy as  $N$  using the algorithm **Train**. In addition, we assume that the time taken by the adversary  $\mathcal{A}$  to break the requirement of unremovability is approximately  $t$ . According to **Game 2**,  $\mathcal{A}$  will output an  $\epsilon$ -accurate model when it is given the knowledge of  $\hat{M}$  and  $vk$ , where at least a  $(1 - \epsilon)$  fraction of the elements in  $V$  are classified correctly by  $\hat{M}$ . We first prove that the adversary's realization of this is independent of the key  $vk$ . To achieve this, we construct a series of algorithms to gradually replace the verification samples in  $vk$  with other random values. Specifically, consider the following algorithm  $\mathcal{S}$ :

1. Generate  $M \leftarrow \mathbf{Train}(\mathcal{O}^f, G)$ .
2. Sample  $(mk, vk) \leftarrow \mathbf{KeyGen}()$ .
3. Compute  $\hat{M} \leftarrow \mathbf{FP}(M, mk)$ .
4. Run  $(\tilde{V}, \tilde{V}_L) = \mathcal{V} \leftarrow \mathbf{F}_{\text{gen}}(\mathcal{O}^f, G)$ , where  $\tilde{V} = \{\tilde{v}^{(1)}, \dots, \tilde{v}^{(n)}\}$  and  $\tilde{V}_L = \{\tilde{v}_L^{(1)}, \dots, \tilde{v}_L^{(n)}\}$ .
5. Set  $c_v^{(1)} \leftarrow \mathbf{Com}(\tilde{v}^{(1)}, h_v^{(1)})$ ,  $c_L^{(1)} \leftarrow \mathbf{Com}(\tilde{v}_L^{(1)}, h_L^{(1)})$ , and  $\tilde{vk} \leftarrow \{c_v^{(i)}, c_L^{(i)}\}_{i \in [n]}$ .
6. Compute  $\hat{M} \leftarrow \mathcal{A}(\mathcal{O}^f, vk, \hat{M})$ .

This algorithm replaces the first element in  $vk$  with an independently generated random element, and then runs  $\mathcal{A}$  on it. Due to the statistical hiding property of **Com**, the output of  $\mathcal{S}$  is statistically close to the output of  $\mathcal{A}$  in the unremovability experiment. Therefore, we can further generate a series of hybrids  $\mathcal{S}^{(2)}, \mathcal{S}^{(3)} \dots, \mathcal{S}^{(n)}$  to change the 2nd to  $n$ -th elements in  $vk$  in the same way. This means that the model  $\hat{M}$  generated by the adversary  $\mathcal{A}$  must be independent of  $vk$ . Based on this, we consider the following algorithm  $\mathcal{T}$ :

1. Compute  $(mk, vk) \leftarrow \mathbf{KeyGen}()$ .
2. Run the adversary and compute  $\hat{N} \leftarrow \mathcal{A}(\mathcal{O}^f, M, vk)$ .

According to the above hybrid argument, the running time of the algorithm  $\mathcal{T}$  is similar to that of  $\mathcal{A}$ , i.e., time  $t$ . Then it generates a model  $\hat{N}$  which does not contain the fingerprint. However, this is contrary to the previous assumption about the persistence of strong fingerprints, i.e.,  $\mathcal{T}$  must also generate an  $\epsilon$ -accurate model given any model in the same time  $t$ .

(IV) **Unforgeability.** Suppose there is a polynomial time algorithm  $\mathcal{A}$  which can break the unforgeability requirement. We use such an algorithm to open the statistically hidden



commitment. Specifically, we design an algorithm  $\mathcal{S}$  which uses  $\mathcal{A}$  as a subroutine. This algorithm trains a regular network (which can be fingerprinted through our scheme) and adds commitments into  $vk$ . Then, it will use  $\mathcal{A}$  to find openings for these commitments.  $\mathcal{S}$  works as follows:

1. Receive the commitments  $c$  from the challenger.
2. Generate  $M \leftarrow \mathbf{Train}(\mathcal{O}^f, G)$ .
3. Sample  $(mk, vk) \leftarrow \mathbf{KeyGen}()$ .
4. Compute  $\hat{M} \leftarrow \mathbf{FP}(M, mk)$ .
5. Let  $vk = \{c_v^{(i)}, c_L^{(i)}\}_{i \in [n]}$ , set  $\hat{c}_v^{(1)} = c$  and  $\hat{c}_v^{(i)} = c_v^{(i)}$  for  $i \in \{2, \dots, n\}$ . Then,  $\hat{v}k \leftarrow \{\hat{c}_v^{(i)}, c_L^{(i)}\}$ .
6. Compute  $(\tilde{M}, \tilde{m}k) \leftarrow \mathcal{A}(\mathcal{O}^f, \hat{v}k, \hat{M})$ .
7. Let  $\tilde{m}k = ((\{v^{(1)}, \dots, v^{(n)}\}, V_L), \{h_v^{(i)}, h_L^{(i)}\}_{i \in [n]})$ . Then, if  $\mathbf{Verify}(\tilde{m}k, \hat{v}k, \tilde{M}) = 1$ , output  $v^{(1)}, h_v^{(1)}$ . Otherwise, output  $\perp$ .

We know that the commitment scheme is statistically hidden, so the input of  $\mathcal{A}$  is statistically indistinguishable from the input where  $\hat{M}$  is fingerprinted on all the committed values of  $vk$ . Therefore, this is statistically indistinguishable between the output of  $\mathcal{A}$  in  $\mathcal{S}$  and the output in the definition of unforgeability. If  $\mathbf{Verify}(\tilde{m}k, \hat{v}k, \tilde{M}) = 1$ , it means that  $\mathbf{Open}(c, v^{(1)}, h_v^{(1)}) = 1$ , so  $v^{(1)}, h_v^{(1)}$  open the challenge commitment  $c$ . Since the commitment is statistically hidden (and the fingerprint we generate is independent of  $c$ ), this will open  $c$  to another value with an overwhelming probability.

*Remark:* The algorithm **Verify** only allows verification by honest parties in a private way. This is evolved from the fact that the key  $mk$  will be known once **Verify** is run, which allows the adversary to retrain the model on the verification sample set. It is not a problem for the applications such as IP protection, because there are trusted third parties in the form of judges. However, for practicality, we may still hope to design a publicly verifiable method without limiting the number of repeated verifications. To achieve this, we can use a powerful cryptographic primitive called the *zero-knowledge proof argument* [10], to convert our fingerprinting scheme from private verifiability to public verifiability. For more details, please refer to Appendix B.

## VII. EXPERIMENTS

### A. Configuration and Implementation

**Model and dataset.** Our scheme can be applied to general GAN models and tasks, since the design does not rely on any assumptions about datasets, model architectures or parameters. Without loss of generality, we employ three mainstream GANs (i.e., AttGAN [20], StarGAN [9], and STGAN [30]) for evaluations, all of which take a face image as input, and produce an image with modified attributes specified by the user. To be precise, we train each model to edit five attributes: black hair, blond hair, brown hair, male and young. We train and test these models on a public face dataset CelebA [31], which is a standard benchmark dataset widely used in this area.

**Scheme implementation.** As described before, we generate and register the fingerprints into a classifier  $\hat{f}$ , and use them to perform copyright verification on a suspicious model that is potentially pirated from the target model. In our experiments,  $\hat{f}$  is implemented by ResNet34 [18], which is widely adopted

TABLE 2: Top-5 attributes for three GANs in generating the verification samples by  $\mathbf{F}_{\text{gen}}$ .

GAN	Selected fingerprinting attributes
AttGAN	Smiling, BagsUnderEyes, Attractive, MouthSlightlyOpen, HighCheekbones
StarGAN	Smiling, Male, Young, WearingNecklace, Attractive
STGAN	BigNose, Young, Smiling, BagsUnderEyes, HighCheekbones

due to its compactness and compatibility with the classification of low-resolution images. Specifically, we train this classifier on the CelebA dataset to predict the facial attributes. Each sample in CelebA has 40 annotated attributes, where we set the resolution of the images to  $128 \times 128$  for simplicity. Note that the construction of  $\hat{f}$  is general, so other mainstream classifier types can also be well applied to our task.

To generate a qualified verification sample set, we uniformly select 100 random samples from the sample space. It guarantees a PPT adversary only has a negligible probability to infer these samples. For each GAN model, 5 facial attributes are selected as the labels to predict (Table 2). We choose them by analyzing the decision boundary of the classifier and finding the easiest attributes to be misclassified. We follow  $\mathbf{F}_{\text{gen}}$  in Algorithm 1 to generate the verification samples  $V$ . Specifically, we minimize the loss function  $F_{obj}$  in Equation 2 under the constraint  $\|G(v^{(i)}), G(x^{(i)})\| \leq \epsilon$ . The value of  $\epsilon$  is set as 0.0009, which is proven to be sufficient to ensure the indistinguishability between the verification sample and its corresponding clean sample. The generated verification sample set can be used for all the three proposed methods.

For CFP-iBDv1 and CFP-iBDv2, we also need to register the fingerprint into the composite model following  $\mathbf{F}_{\text{reg}}$  in Algorithm 2. We fix  $\mathcal{G}$ , while fine-tuning the classifier  $f$  using the prepared verification sample set. This will give us the final fingerprint-registered composite model  $\hat{M} = f(\mathcal{G}(\cdot))$ . To enhance the robustness of the fingerprinted classifier, we adopt four types of mainstream image transformations (adding noise, blurring, compression and cropping) to augment the verification sample set  $\mathcal{V}_s$  and normal sample set  $\mathcal{N}_s$ .

For verification, we query the suspicious GAN model with the 100 verification samples. We feed the received responses to the classifier  $\hat{f}$  and check whether the predicted attributes match the verification labels. When the ratio of matched verification sample-label pairs is higher than a pre-defined threshold  $\tau$  (0.8 in our experiments), we have confidence to claim that the suspicious model is a pirated version.

**Baselines.** Since the GAN image attribution methods are either vulnerable to model retraining with different data samples [48], or require model modifications [49], [50], we do not consider applying them for GAN fingerprinting. We mainly migrate the fingerprinting solutions from classification models to GANs as our baselines. As discussed in Section II, we adopt two common strategies to directly generate adversarial examples from the target model as verification samples. (1) AE-D leverages the *distortion attack* [14], [23], [36], [37], [47] to generate adversarial examples, whose outputs are distorted away from the correct one. The adversary generates such perturbations by maximizing the distance between the adversarial output and ground-truth output. During verification, we use such samples

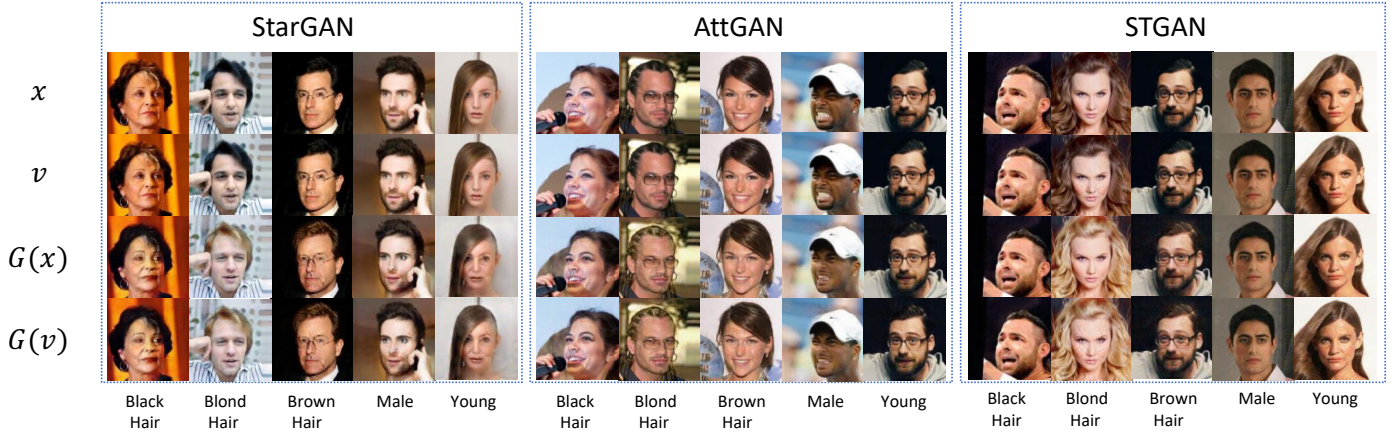


Fig. 5: Fingerprint visualization for three GAN models with five edited attributes. (a) Clean sample  $x$ ; (b) Verification sample  $v$ ; (c) GAN output of clean sample  $G(x)$ ; (d) GAN output of verification sample  $G(v)$ .

to query the suspicious model and determine its legitimacy by measuring the noise ratio of the responses and ground-truth outputs. A model is considered as illegal if the peak signal-to-noise ratio (PSNR) [21] is smaller than a threshold (20 in this paper). (2) AE-I leverages the *identity attack* [37], [47] to generate adversarial examples, whose outputs are identical with the inputs. This is achieved by minimizing the distance between the sample outputs and inputs. During verification, we determine the legitimacy of the suspicious model by measuring the similarity between the verification samples and the corresponding responses. We flag the model as pirated if their Euclidean distance is smaller than a threshold (0.0009 in this paper). Both types of adversarial examples are generated by the state-of-the-art C&W technique [5], which is also considered in [4] for fingerprinting classification models.

**Metrics.** A good fingerprinted model should show high accuracy on both the verification samples and normal samples, and ensure that the non-target model has poor accuracy on the verification samples. We introduce two metrics: (1) Match Score for Verification samples (MSV) denotes the matching ratio of verification labels for verification samples; (2) Match Score for Clean samples (MSC) denotes the matching ratio of ground-truth labels for clean samples. For a good fingerprinting scheme, the target model should have high MSV and MSC, while the MSV on non-target models should be very low.

In the following, we conduct experiments on all the methods (AE-D, AE-I, CFP-AE, CFP-iBDv1, CFP-iBDv2) to assess different requirements. The requirements of non-trivial ownership and unforgeability are bound to the security of the cryptographic primitives we use, and we have provided theoretical proofs for them in Section VI. Here, we mainly experimentally evaluate the other three requirements. We will show that our scheme is better than the prior strategy, and CFP-iBDv2 gives the most satisfactory performance.

### B. Stealthiness Analysis

A qualified fingerprinting scheme should ensure that the verification process is indistinguishable from normal inference. In Section II, we have shown some results about the possibility of detecting verification samples based on adversarial examples. Additionally, we consider the stealthiness property from

another two directions. Given a verification sample  $v$  generated from a clean one  $x$ , the distance  $\mathcal{H} = \|v, x\| + \|G(v), G(x)\| + \sum_j \|G_{v,j}, G_{x,j}\|$  should be small enough. We demonstrate the sample space indistinguishability for the distances  $\|v, x\|$  and  $\|G(v), G(x)\|$ , as well as the feature space indistinguishability for the distance  $\|G_{v,j}, G_{x,j}\|$ . Note that all our three methods share the same verification samples since they use the same  $\mathbf{F}_{\text{gen}}$ . So we use CFP-\* to represent any of our methods.

**Sample space indistinguishability.** Fig. 5 visually compares the verification query-response images with the ground-truth (normal images) for our proposed methods CFP-\*. We observe that the perturbations added to the verification samples and model output samples are imperceptible. This confirms that the objective function enforced in the process of generating verification samples is effective and achieves the expected results. Moreover, Table 3 quantitatively shows the peak signal-to-noise ratio (PSNR) and structural similarity (SSIM) [21] between the input of clean and verification samples, as well as between their output samples. These two metrics are widely used in computer vision to measure the similarity of images: two pictures with  $\text{PSNR} > 35$  or  $\text{SSIM} > 0.95$  are generally considered to be the same in human vision. Although AE-I and AE-D have indistinguishability for the input samples, their output images are significantly different from ground-truth ones. In contrast, our verification samples meet the visual indistinguishability from normal samples for both model inputs and outputs. This improves the concealment of copyright verification and makes it difficult for adversaries to distinguish verification samples from visual changes.

**Feature space indistinguishability.** An adversary may try to monitor the intermediate results (e.g., feature maps) of the inference process to detect the verification samples. Anomalous samples usually result in unique behaviors in the feature space, which has been exploited to detect adversarial attacks [25], [27], [42]. Specifically, we produce 100 samples for each category (normal, AE-I, AE-D, and CFP-\*). We compute the standard deviation of feature maps for each sample, and then the cumulative probabilities among these 100 samples in one category. If the cumulative probability distribution of one category is closer to that of normal samples, it will be

<sup>3</sup>Visualizations of AE-I and AE-D can be found in Appendix C

TABLE 3: PSNR and SSIM of the verification and clean input ( $v, x$ ) and output ( $G(v), G(x)$ ) images for different edited attributes. A1: Black Hair. A2: Blond Hair. A3: Brown Hair. A4: Male. A5: Young. (“-” in AE-D indicates we are not able to find the qualified verification samples using the algorithm  $F_{\text{gen}}$ .)

Similarity		StarGAN					AttGAN					STGAN				
		A1	A2	A3	A4	A5	A1	A2	A3	A4	A5	A1	A2	A3	A4	A5
PSNR( $v, x$ )	AE-I	43.84	43.73	43.64	43.72	43.99	39.92	38.68	38.65	39.60	40.07	38.27	38.23	39.50	39.73	39.36
	AE-D	33.62	33.67	33.68	33.57	-	33.70	33.72	33.62	34.09	34.24	33.35	33.81	33.67	-	33.39
	CFP-*	41.54	42.38	42.34	41.12	40.86	47.50	45.54	46.41	46.16	46.41	46.22	44.08	43.48	44.56	44.64
SSIM( $v, x$ )	AE-I	0.99	0.99	0.99	0.99	0.99	0.96	0.95	0.95	0.96	0.96	0.97	0.97	0.98	0.97	0.98
	AE-D	0.89	0.89	0.89	0.89	-	0.90	0.90	0.90	0.91	0.90	0.90	0.90	0.91	-	0.94
	CFP-*	0.98	0.98	0.98	0.98	0.98	0.99	0.99	0.99	0.99	0.99	0.99	0.99	0.99	0.99	0.99
PSNR( $G(v), G(x)$ )	AE-I	22.44	18.28	23.37	24.59	23.98	30.83	27.79	29.04	29.43	29.66	31.78	33.82	36.32	37.29	36.87
	AE-D	10.99	10.07	10.85	10.77	-	23.94	22.92	24.51	25.65	28.29	22.50	20.12	25.71	-	29.62
	CFP-*	37.75	38.00	38.12	37.37	37.20	45.33	43.33	44.38	44.46	44.36	44.53	42.78	42.81	43.94	44.01
SSIM( $G(v), G(x)$ )	AE-I	0.84	0.79	0.87	0.87	0.85	0.95	0.92	0.92	0.94	0.94	0.96	0.97	0.98	0.98	0.98
	AE-D	0.40	0.38	0.41	0.40	-	0.86	0.85	0.87	0.89	0.90	0.85	0.84	0.90	-	0.93
	CFP-*	0.97	0.97	0.97	0.96	0.96	0.99	0.99	0.99	0.99	0.99	0.99	0.99	0.99	0.99	0.99

TABLE 4: The cumulative probability of the standard deviation of feature maps for different types of samples.

Method	Standard deviation of feature maps							
	0.650	0.675	0.700	0.725	0.750	0.775	0.800	0.825
Normal	0%	3%	9%	15%	38%	63%	92%	100%
AE-I	0%	2%	19%	58%	97%	100%	100%	100%
AE-D	0%	18%	64%	99%	100%	100%	100%	100%
CFP-*	0%	3%	14%	37%	69%	86%	98%	100%

harder for the adversary to identify such verification samples in the feature space. Table 4 shows the statistical results for these fingerprinting solutions. Obviously, the stealthiness of the verification samples generated by CFP-\* is much better than that of AE-I and AE-D since its distribution is closer to the normal one’s. This stems from the comprehensiveness of CFP-\* in generating verification samples. To be precise, compared with AE-I and AE-D, the construction of our verification samples is forced to minimize the distance  $\|G_{v,j}, G_{x,j}\|$ . It fundamentally ensures the consistency of the distribution in the feature space between verification and normal samples.

### C. Functionality-preserving Analysis

A fine-tuned model  $\hat{M} = \hat{f}(G(x))$  should be functionally preserved, which means it can predict the desired labels for both verification samples and normal samples. Meanwhile, we also require the verification samples to exclusively match the composite model: a different GAN model or classifier will still predict normal labels for the verification samples. In the following, we construct experiments to compare the performance of these fingerprinting schemes from two aspects.

**GAN uniqueness.** We generate verification samples from one target GAN model, and use them to verify the model itself, as well as other non-target GAN models, including a model trained with the same configurations (network structure, algorithm, hyper-parameters and dataset). Table 5 shows the Match Scores for different models. We observe that all methods perform well on the target model (the “Target GAN” column). For other non-target models, AE-I performs the best in reducing the false positives. This indicates the adversarial identity attack has much lower transferability to other models. We will later show that AE-I is impractical in terms of unremovability (Section VII-D). AE-D has high transferability for StarGAN, hence it fails to distinguish target and non-target GAN models trained from the same StarGAN algorithm. Our proposed methods are generally fair to distinguish target and

non-target models with a threshold  $\tau = 0.8$ . CFP-iBDv2 is better than CFP-AE and CFP-iBDv1, due to the utilization of more sophisticated loss functions when fine-tuning the classifier. For instance, we adopt  $\mathcal{L}_{G2}$  to maximize the distance between verification sample responses and normal sample responses, making  $\hat{f}$  predict correct labels more easily.

**Classifier uniqueness.** Our fingerprinting scheme is also exclusive for the classifier  $\hat{f}$ . To demonstrate this, we replace  $\hat{f}$  in the composite model with other classifiers of the same architecture (ResNet34 trained from scratch) or different architectures (MobileNetv2, VGG19). Table 5 summarizes the results<sup>4</sup>. We observe that CFP-iBDv1 and CFP-iBDv2 demonstrate better uniqueness for the classifier than CFP-AE<sup>5</sup>. This stems from the following two arguments. First, the generated adversarial examples from the GAN model have high transferability over different classifiers, so they have higher chances to pass the composite models with a different classifier. Second, the backdoor samples are generally unique for the classifier embedded with the backdoor. Hence, the outputs of the GAN model for the verification samples from CFP-iBDv1 and CFP-iBDv2 are exclusively recognized by the classifier during the fine-tuning process.

### D. Unremovability Analysis

Unremovability means that a fingerprinting scheme should be also effective even if the adversary makes certain modifications to the inference process while maintaining its correctness. In our experiments, we consider a PPT adversary who performs the following two types of modifications in an attempt to invalidate fingerprint verification: (1) we adopt mainstream techniques (e.g., pruning and fine-tuning) to alter the GAN model in a lightweight way, which are also widely used to analyze the unremovability of watermarks or fingerprints in classification models. (2) We use popular image preprocessing operations (e.g., blurring, cropping, adding noise and compression) to modify the output of the GAN model, which can potentially alter the verification results from the classifier.

**Unremovability against model transformations.** We consider two model transformation methods. (1) For model fine-tuning, we refine the model with different epochs (10, 20

<sup>4</sup>We do not consider AE-I and AE-D since they do not need a classifier.

<sup>5</sup>Since we only replace the classifier without changing the GAN model, the verification samples generated by CFP-iBDv1 and CFP-iBDv2 are consistent, so are the Match scores.

TABLE 5: MSC (%) and MSV (%) for verifying different GAN models and classifiers.  $\downarrow$  means a lower score is better.  $\uparrow$  means a higher score is better. Same for the following tables.

GAN Structure	Method	Target GAN		Non-target GAN						Other classifier					
		MSC $\uparrow$	MSV $\uparrow$	StarGAN		AttGAN		STGAN		ResNet34		MobileNetv2		VGG19	
				MSC $\uparrow$	MSV $\downarrow$	MSC $\uparrow$	MSV $\downarrow$	MSC $\uparrow$	MSV $\downarrow$	MSC $\uparrow$	MSV $\downarrow$	MSC $\uparrow$	MSV $\downarrow$	MSC $\uparrow$	MSV $\downarrow$
StarGAN	AE-I	100.00	100.00	100.00	0.00	100.00	0.00	99.00	0.00	-	-	-	-	-	-
	AE-D	100.00	100.00	97.00	100.00	82.00	20.00	89.00	12.00	-	-	-	-	-	-
	CFP-AE	100.00	100.00	95.80	50.20	82.60	33.80	89.00	30.40	94.20	62.00	92.20	54.20	92.80	53.20
	CFP-iBDv1	95.52	94.12	84.00	62.10	89.45	15.10	86.15	27.00	96.15	9.92	96.05	9.07	96.58	8.85
	CFP-iBDv2	92.87	90.05	88.55	39.62	89.15	12.53	89.75	16.92	96.15	9.92	96.05	9.07	96.58	8.85
AttGAN	AE-I	100.00	100.00	100.00	0.00	100.00	0.00	100.00	0.00	-	-	-	-	-	-
	AE-D	100.00	14.00	82.00	35.00	100.00	1.00	94.00	6.00	-	-	-	-	-	-
	CFP-AE	100.00	100.00	88.00	29.00	93.00	42.20	93.60	39.80	94.20	59.00	92.40	51.40	93.00	51.40
	CFP-iBDv1	93.40	92.45	69.13	49.10	90.70	34.20	76.45	57.02	96.35	9.72	96.05	9.07	95.58	9.05
	CFP-iBDv2	91.03	90.70	83.18	27.15	89.13	17.85	87.43	30.10	96.35	9.72	96.05	9.07	95.58	9.05
STGAN	AE-I	98.00	100.00	100.00	0.00	100.00	0.00	99.00	13.00	-	-	-	-	-	-
	AE-D	100.00	34.00	69.00	66.00	79.00	22.00	100.00	1.00	-	-	-	-	-	-
	CFP-AE	100.00	100.00	91.40	26.20	94.20	25.80	99.00	67.80	94.60	32.80	92.40	29.60	96.40	27.00
	CFP-iBDv1	93.53	91.57	82.13	50.52	89.08	42.08	92.00	83.20	96.55	10.67	96.68	9.22	96.40	9.75
	CFP-iBDv2	92.20	90.18	87.73	30.05	88.80	28.75	91.20	69.05	96.55	10.67	96.68	9.22	96.40	9.75

and 30) using the same training set. Such a setting is commonly used in previous works, and also in line with the adversary’s capability in this paper, i.e., a party with limited computing power. (2) For model pruning, we consider two compression ratios (0.2 and 0.4). Experimental results show that a compression ratio higher than 0.4 can lead to significant accuracy degradation for GAN models (see Appendix D-B), which is impractical for the adversary to perform. As shown in Table 6, AE-I can hardly resist these transformations from the adversary. This is due to the fact that the above attacks will fundamentally change the generation details of the target model, while the effectiveness of AE-I highly depends on the invariance of these details. AE-D will benefit from these model operations, which can further distort the model output and decrease the PSNR value. But this is still not enough for verifying AttGAN and STGAN. In contrast, our methods achieve satisfactory robustness under these modifications.

**Unremovability against image transformations.** The adversary may adopt image transformations to process the model outputs, making the verification samples unrecognizable by the classifier. We consider four common transformations: *adding Gaussian noises* (with mean  $\mu = 0$  and standard deviation  $\sigma = 0.1$ ), *Gaussian blurring* (with a kernel size of 5), *JPEG compression* (with a compression ratio of 35%), and *center cropping* (from  $128 \times 128$  to  $100 \times 100$ ). These transformations will still maintain the quality of the images. Table 7 reports the Match scores. Similarly, we observe AE-I is not robust at all, as these operations can significantly compromise the details of the images and invalidate the verification process. For our approach, CFP-AE is less effective for STGAN models. This is because the output of STGAN is more sensitive than other models, due to its adaptive selection structure, which gives more details in the output. In contrast, CFP-iBDv1 and CFP-iBDv2 perform the best, as the backdoor classifier together with the invisible backdoor samples are more robust against these image operations, further enhanced by the data augmentation during fingerprint registration. We also measure the impacts of different transformation strengths on the fingerprint verification, and the results are reported in Appendix D-B.

### E. Summary

Table 8 summarizes the comparisons of those methods from the above evaluations. There are five levels to assess

each property of each method. We conclude that AE-I and AE-D are not stealthy, especially from the feature space. This gives an adversary more chances to detect the verification samples and manipulate the results, which is also demonstrated in Section II. AE-I is unique for the GAN model, but not robust enough against model pruning, fine-tuning or image transformations. Although AE-D achieves good uniqueness on StarGAN, it cannot guarantee the high quality of verification samples on other GAN models, leading to low MSV scores. In Appendix C, we show the outputs of verification samples for three GANs, which reveal that AE-D is not a stable and general fingerprinting method.

Our proposed scheme and methods give much better stealthiness in both the sample space and feature space. CFP-AE does not show high capabilities of distinguishing classifiers, or resisting image transformations. With the introduction of the invisible backdoor technique for fingerprint registration, CFP-iBDv1 and CFP-iBDv2 can significantly improve the effectiveness and unremovability. The two novel loss function terms in CFP-iBDv2 can further increase the distinguishability between target and non-target GAN models.

## VIII. RELATED WORKS

**Watermarking DNN models.** This technology is to embed watermarks into the target DNN models for ownership verification. Existing schemes can be classified into two categories: (1) parameter-embedding solutions [6], [35], [41] inject watermarks into the model parameters while preserving the model performance. For example, [41] embedded a bit-vector (signature) into the model parameters via a carefully-designed parameter regularizer. (2) Data-poisoning solutions take a set of unique sample-label pairs as watermarks and embed their correlation into the model during training. To preserve the fidelity and robustness of the watermarked models, the essential part of these solutions is the generation of watermark samples. For example, [2], [52] leveraged the DNN backdoor attacks to embedded backdoor samples with certain trigger patterns into the models; [26], [29] adopted imperceptible perturbations as the verification samples. Chen et al. [7] designed temporal state sequences to watermark reinforcement learning models. Lou et al. [45] utilized cache side channels to verify watermarks embedded in the model architecture.

However, these solutions were empirically proven to be

TABLE 6: MSC (%) and MSV (%) after model transformations (fine-tuning and pruning) with different configurations.

GAN Structure	Method	Target GAN		Fine-tuning (epochs)						Pruning (compression ratio)			
				10		20		30		0.2		0.4	
		MSC $\uparrow$	MSV $\uparrow$	MSC $\uparrow$	MSV $\uparrow$	MSC $\uparrow$	MSV $\uparrow$	MSC $\uparrow$	MSV $\uparrow$	MSC $\uparrow$	MSV $\uparrow$	MSC $\uparrow$	MSV $\uparrow$
StarGAN	AE-I	100.00	100.00	100.00	0.00	100.00	6.00	100.00	2.00	100.00	43.00	100.00	0.00
	AE-D	100.00	100.00	100.00	100.00	99.00	100.00	100.00	100.00	100.00	100.00	100.00	100.00
	CFP-AE	100.00	100.00	96.60	94.20	96.40	91.80	97.00	96.00	98.80	98.20	94.60	97.00
	CFP-iBDv1	95.52	94.12	94.98	93.07	92.20	89.25	92.88	92.15	95.58	94.12	95.35	93.60
	CFP-iBDv2	92.87	90.05	92.53	85.32	92.28	84.57	92.68	84.80	92.73	90.02	92.78	89.57
AttGAN	AE-I	100.00	100.00	100.00	91.00	100.00	84.00	100.00	75.00	100.00	22.00	100.00	0.00
	AE-D	100.00	14.00	100.00	14.00	100.00	14.00	100.00	14.00	100.00	14.00	100.00	16.00
	CFP-AE	100.00	100.00	98.60	94.60	99.80	95.40	99.00	94.80	97.80	91.20	86.40	87.40
	CFP-iBDv1	93.40	92.45	93.33	92.37	93.45	92.40	93.45	92.37	93.53	92.40	93.08	89.00
	CFP-iBDv2	91.03	90.70	91.93	90.62	92.00	90.70	92.05	90.67	91.98	90.75	91.95	84.95
STGAN	AE-I	98.00	100.00	100.00	85.00	99.00	75.00	92.00	73.00	100.00	58.00	100.00	0.00
	AE-D	100.00	34.00	100.00	36.00	100.00	36.00	100.00	32.00	100.00	34.00	100.00	57.00
	CFP-AE	100.00	100.00	99.40	95.40	99.80	95.20	99.40	94.60	98.60	95.00	93.40	86.60
	CFP-iBDv1	93.53	91.57	93.58	91.62	93.53	91.72	93.28	91.80	93.38	91.45	84.20	91.40
	CFP-iBDv2	92.20	90.18	92.08	90.30	92.20	90.25	91.95	90.40	91.55	90.22	88.98	83.35

TABLE 7: MSC (%) and MSV (%) after four image transformations.

GAN Structure	Method	Target GAN		Image Transformation									
				Noise		Blur		Compression		Crop			
		MSC $\uparrow$	MSV $\uparrow$	MSC $\uparrow$	MSV $\uparrow$	MSC $\uparrow$	MSV $\uparrow$	MSC $\uparrow$	MSV $\uparrow$	MSC $\uparrow$	MSV $\uparrow$		
StarGAN	AE-I	100.00	100.00	100.00	1.00	100.00	0.00	100.00	0.00	100.00	0.00	100.00	0.00
	AE-D	100.00	100.00	100.00	100.00	100.00	100.00	100.00	100.00	100.00	100.00	3.00	100.00
	CFP-AE	100.00	100.00	67.20	77.60	83.20	84.60	89.20	89.00	80.00	81.60	80.00	81.60
	CFP-iBDv1	95.52	94.12	94.75	93.12	94.85	93.57	95.03	93.75	95.03	93.57	95.03	93.57
	CFP-iBDv2	92.87	90.05	92.83	86.02	92.05	87.57	92.30	89.70	92.25	90.62	92.25	90.62
AttGAN	AE-I	100.00	100.00	100.00	1.00	100.00	0.00	100.00	0.00	100.00	0.00	100.00	0.00
	AE-D	100.00	14.00	100.00	18.00	100.00	14.00	100.00	14.00	100.00	14.00	4.00	97.00
	CFP-AE	100.00	100.00	67.20	82.00	80.20	73.00	86.80	84.80	67.60	76.80	67.60	76.80
	CFP-iBDv1	93.40	92.45	92.60	91.20	92.75	92.07	92.90	92.52	92.90	92.52	93.33	91.57
	CFP-iBDv2	91.03	90.70	91.38	80.32	91.40	84.10	91.58	89.30	91.58	88.82	91.58	88.82
STGAN	AE-I	98.00	100.00	100.00	0.00	100.00	0.00	100.00	0.00	100.00	0.00	100.00	0.00
	AE-D	100.00	34.00	100.00	41.00	100.00	39.00	100.00	36.00	100.00	36.00	2.00	100.00
	CFP-AE	100.00	100.00	85.50	77.00	94.80	41.20	96.00	65.20	84.20	57.00	84.20	57.00
	CFP-iBDv1	93.53	91.57	92.53	89.00	92.98	90.72	93.30	91.45	93.48	90.95	93.48	90.95
	CFP-iBDv2	92.20	90.18	91.53	86.40	91.48	86.55	91.75	88.15	91.58	88.80	91.58	88.80

TABLE 8: Assessment of each fingerprinting method for each property. Rating scores: Excellent > Good > Fair > Poor > Bad.

Method	Stealthiness		Functionality-preserving		Unremovability	
	Sample space	Feature space	GAN uniqueness	Classifier uniqueness	Model transformations	Image transformations
AE-I	Fair	Bad	Excellent	-	Bad	Bad
AE-D	Poor	Bad	Poor	-	Fair	Fair
CFP-AE	Excellent	Good	Poor	Poor	Excellent	Good
CFP-iBDv1	Excellent	Good	Fair	Excellent	Excellent	Excellent
CFP-iBDv2	Excellent	Good	Good	Excellent	Excellent	Excellent

vulnerable to watermark removal attacks [8], [17], [39]. Besides, embedding watermarks into the model requires the parameter changes, which can compromise the model performance to some extent [4]. These limitations can be addressed by DNN fingerprinting, as considered in this paper.

**Fingerprinting DNN models.** Some works proposed fingerprinting schemes for classification models. They leveraged adversarial examples as fingerprints to identify the target models. For example, IPGuard [4] identified the data samples close to the target model’s decision boundary to fingerprint this model. [32] adopted conferrable adversarial examples with certain labels, which can transfer from the target model to its surrogates, while remaining ineffective to other non-target models. A prior work [19] designed sensitive samples to fingerprint black-box models, which will fail even the model has very small modifications.

In this paper, we focus on fingerprinting the more complicated GANs. Due to the fundamental differences between classification and GAN models, these methods cannot be easily extended to achieve our goal. Our novel scheme can signifi-

cantly extend the IP protection scope and demonstrate much stronger stealthiness and robustness under various scenarios than prior solutions.

**Detection and attribution of GAN-generated images by fingerprinting.** Some works leveraged the fingerprint concept to detect GAN-generated images and trace their sources [48], [49], [50]. The key idea is that a GAN model can leave some fingerprints in its outputs. By extracting the fingerprint from an image, one can identify which model generates it. However, these solutions are not quite applicable to fingerprint GAN models for IP protection. For instance, the solutions in [49], [50] require the model owner to modify the GAN model to have the capability of embedding fingerprints in the output images, which violates the requirement of model fingerprinting (they should be treated as watermarking more rigorously). The method in [48] does not need to process the target GAN model. However, the fingerprint in the output image is very sensitive to model transformations: “Even GAN training sets that differ in just one image can lead to distinct GAN instances [48].” As a result, an adversary can just use a different training set to

fine-tune the target GAN model to invalidate the fingerprint. In contrast, our methods do not need to modify the model, and exhibit higher unremovability.

## IX. CONCLUSION

We propose a novel scheme to fingerprint GAN models and protect their copyright. We introduce a classifier to construct a composite model with the protected GAN. From this composite model, we craft verification samples as the fingerprint, and register it in the classifier. The classifier is able to distinguish the target and non-target models in a stealthy and robust manner. We design three fingerprinting methodologies based on generative adversarial examples and invisible backdoor attacks. Theoretical proof and empirical evaluations validate the effectiveness of our designs. In the future, we will explore more techniques and methodologies following this scheme to further enhance the fingerprinting solutions, and apply them to different types of GAN models and domains.

## REFERENCES

- [1] M. Abdalla, J. H. An, M. Bellare, and C. Namprempre, "From identification to signatures via the fiat-shamir transform: Minimizing assumptions for security and forward-security," in *Proc. of the Eurocrypt*, 2002, pp. 418–433. [18](#)
- [2] Y. Adi, C. Baum, M. Cisse, B. Pinkas, and J. Keshet, "Turning your weakness into a strength: Watermarking deep neural networks by backdooring," in *Proc. of the USENIX Security*, 2018, pp. 1615–1631. [1](#), [2](#), [5](#), [12](#)
- [3] A. Brock, J. Donahue, and K. Simonyan, "Large scale GAN training for high fidelity natural image synthesis," in *Proc. of the ICLR*, 2019. [1](#)
- [4] X. Cao, J. Jia, and N. Z. Gong, "IPGuard: Protecting the intellectual property of deep neural networks via fingerprinting the classification boundary," *CoRR*, vol. abs/1910.12903, 2019. [1](#), [2](#), [6](#), [10](#), [13](#)
- [5] N. Carlini and D. Wagner, "Towards evaluating the robustness of neural networks," in *Proc. of the S&P*, 2017, pp. 39–57. [3](#), [10](#)
- [6] H. Chen, B. D. Rohani, and F. Koushanfar, "DeepMarks: A digital fingerprinting framework for deep neural networks," *CoRR*, vol. abs/1804.03648, 2018. [12](#)
- [7] K. Chen, S. Guo, T. Zhang, S. Li, and Y. Liu, "Temporal watermarks for deep reinforcement learning models," in *Proc. of the AAMAS*, 2021. [12](#)
- [8] X. Chen, W. Wang, C. Bender, Y. Ding, R. Jia, B. Li, and D. Song, "REFIT: A unified watermark removal framework for deep learning systems with limited data," in *Proc. of the AsiaCCS*, 2019. [13](#)
- [9] Y. Choi, M. Choi, M. Kim, J.-W. Ha, S. Kim, and J. Choo, "StarGAN: Unified generative adversarial networks for multi-domain image-to-image translation," in *Proc. of the CVPR*, 2018, pp. 8789–8797. [2](#), [3](#), [9](#)
- [10] A. Coladangelo, T. Vidick, and T. Zhang, "Non-interactive zero-knowledge arguments for qma, with preprocessing," in *Proc. of the Crypto*, 2020, pp. 799–828. [9](#), [17](#)
- [11] J. Deng, J. Krause, and L. Fei-Fei, "Fine-grained crowdsourcing for fine-grained recognition," in *Proc. of the CVPR*, 2013, pp. 580–587. [2](#), [7](#)
- [12] C. Donahue, J. McAuley, and M. Puckette, "Adversarial audio synthesis," *CoRR*, vol. abs/1802.04208, 2018. [1](#)
- [13] A. Dubey, O. Gupta, R. Raskar, and N. Naik, "Maximum-Entropy Fine Grained Classification," in *Proc. of the NeurIPS*, 2018, pp. 635–645. [7](#)
- [14] Z. Fang, Y. Yang, J. Lin, and R. Zhan, "Adversarial attacks for multi target image translation networks," in *Proc. of the PIC*, 2020, pp. 179–184. [3](#), [9](#)
- [15] E. Gavves, B. Fernando, C. G. Snoek, A. W. Smeulders, and T. Tuytelaars, "Fine-grained categorization by alignments," in *Proc. of the ICCV*, 2013, pp. 1713–1720. [2](#), [7](#)
- [16] I. J. Goodfellow, J. Pouget-Abadie, M. Mirza, B. Xu, D. Warde-Farley, S. Ozair, A. C. Courville, and Y. Bengio, "Generative Adversarial Nets," in *Proc. of the NeurIPS*, 2014, pp. 2672–2680. [1](#)
- [17] S. Guo, T. Zhang, H. Qiu, Y. Zeng, T. Xiang, and Y. Liu, "Fine-tuning is not enough: A simple yet effective watermark removal attack for dnn models," in *Proc. of the IJCAI*, 2021. [13](#)
- [18] K. He, X. Zhang, S. Ren, and J. Sun, "Deep residual learning for image recognition," in *Proc. of the CVPR*, 2016, pp. 770–778. [3](#), [9](#)
- [19] Z. He, T. Zhang, and R. Lee, "Sensitive-sample fingerprinting of deep neural networks," in *Proc. of the CVPR*, 2019, pp. 4729–4737. [13](#)
- [20] Z. He, W. Zuo, M. Kan, S. Shan, and X. Chen, "AttGAN: Facial attribute editing by only changing what you want," *IEEE Transactions on Image Processing*, vol. 28, no. 11, pp. 5464–5478, 2019. [1](#), [2](#), [9](#)
- [21] A. Horé and D. Ziou, "Image quality metrics: Psnr vs. ssim," in *Proc. of the ICPR*, 2010, pp. 2366–2369. [10](#)
- [22] W. Hu, M. Wang, Q. Qin, J. Ma, and B. Liu, "HRN: A holistic approach to one class learning," in *Proc. of the NeurIPS*, 2020. [3](#)
- [23] Q. Huang, J. Zhang, W. Zhou, W. Zhang, and N. Yu, "Initiative defense against facial manipulation," in *Proc. of the AAI*, 2021, pp. 1619–1627. [3](#), [9](#)
- [24] A. Juels and M. Wattenberg, "A fuzzy commitment scheme," in *Proc. of the CCS*, 1999, pp. 28–36. [4](#), [5](#)
- [25] Z. Katzir and Y. Elovici, "Detecting adversarial perturbations through spatial behavior in activation spaces," in *Proc. of the IJCNN*, 2019, pp. 1–9. [10](#)
- [26] E. Le Merrer, P. Perez, and G. Trédan, "Adversarial frontier stitching for remote neural network watermarking," *Neural Computing and Applications*, pp. 1–12, 2019. [1](#), [12](#)
- [27] K. Lee, K. Lee, H. Lee, and J. Shin, "A Simple Unified Framework for Detecting Out-of-Distribution Samples and Adversarial Attacks," in *Proc. of the NeurIPS*, 2018, pp. 7167–7177. [10](#)
- [28] S. Li, B. Z. H. Zhao, J. Yu, M. Xue, D. Kaafar, and H. Zhu, "Invisible backdoor attacks against deep neural networks," *CoRR*, vol. abs/1909.02742, 2019. [2](#), [7](#)
- [29] Z. Li, C. Hu, Y. Zhang, and S. Guo, "How to prove your model belongs to you: A blind-watermark based framework to protect intellectual property of DNN," in *Proc. of the ACSAC*, 2019, pp. 126–137. [1](#), [12](#)
- [30] M. Liu, Y. Ding, M. Xia, X. Liu, E. Ding, W. Zuo, and S. Wen, "STGAN: A unified selective transfer network for arbitrary image attribute editing," in *Proc. of the CVPR*, 2019, pp. 3673–3682. [2](#), [9](#)
- [31] Z. Liu, P. Luo, X. Wang, and X. Tang, "Deep learning face attributes in the wild," in *Proc. of the ICCV*, 2015, pp. 3730–3738. [9](#)
- [32] N. Lukas, Y. Zhang, and F. Kerschbaum, "Deep neural network fingerprinting by conferrable adversarial examples," *CoRR*, vol. abs/1912.00888, 2019. [1](#), [2](#), [6](#), [13](#)
- [33] W. Luo, X. Yang, X. Mo, Y. Lu, L. Davis, J. Li, J. Yang, and S.-N. Lim, "Cross-X Learning for Fine-Grained Visual Categorization," in *Proc. of the ICCV*, 2019, pp. 8241–8250. [7](#)
- [34] S. Reed, Z. Akata, X. Yan, L. Logeswaran, B. Schiele, and H. Lee, "Generative adversarial text to image synthesis," in *Proc. of the ICML*, 2016, pp. 1060–1069. [1](#)
- [35] B. D. Rouhani, H. Chen, and F. Koushanfar, "Deepsigns: An end-to-end watermarking framework for protecting the ownership of deep neural networks," in *Proc. of the ASPLOS*, 2019. [12](#)
- [36] N. Ruiz, S. A. Bargal, and S. Sclaroff, "Disrupting deepfakes: Adversarial attacks against conditional image translation networks and facial manipulation systems," in *Proc. of the ECCV Workshops*, 2020, pp. 236–251. [3](#), [9](#)
- [37] —, "Protecting against image translation deepfakes by leaking universal perturbations from black-box neural networks," *CoRR*, vol. abs/2006.06493, 2020. [3](#), [9](#), [10](#)
- [38] F. Schroff, D. Kalenichenko, and J. Philbin, "FaceNet: A unified embedding for face recognition and clustering," in *Proc. of the CVPR*, 2015, pp. 815–823. [2](#), [7](#)
- [39] M. Shafieinejad, N. Lukas, J. Wang, X. Li, and F. Kerschbaum, "On the robustness of backdoor-based watermarking in deep neural networks," in *Proc. of the ACM Workshop on Information Hiding and Multimedia Security*, 2021, pp. 177–188. [13](#)
- [40] G. Sun, S. Ding, T. Sun, and C. Zhang, "Sa-capsgan: Using capsule networks with embedded self-attention for generative adversarial network," *Neurocomputing*, vol. 423, pp. 399–406, 2021. [1](#)
- [41] Y. Uchida, Y. Nagai, S. Sakazawa, and S. Satoh, "Embedding watermarks into deep neural networks," in *Proc. of the ICMR*, 2017, pp. 269–277. [1](#), [12](#)
- [42] J. Wang, G. Dong, J. Sun, X. Wang, and P. Zhang, "Adversarial sample detection for deep neural network through model mutation testing," in *Proc. of the ICSE*, 2019, pp. 1245–1256. [10](#)
- [43] T.-C. Wang, M.-Y. Liu, J.-Y. Zhu, A. Tao, J. Kautz, and B. Catanzaro, "High-resolution image synthesis and semantic manipulation with conditional gans," in *Proc. of the CVPR*, 2018, pp. 8798–8807. [1](#)
- [44] C. Xiao, B. Li, J.-Y. Zhu, W. He, M. Liu, and D. Song, "Generating adversarial examples with adversarial networks," in *Proc. of the IJCAI*, 2018, pp. 3905–3911. [6](#)
- [45] L. Xiaoxuan, G. Shangwei, Z. Tianwei, L. Yang *et al.*, "When nas meets watermarking: Ownership verification of dnn models via cache side channels," *CoRR*, vol. abs/2102.03523, 2021. [12](#)
- [46] Z. Yang, T. Luo, D. Wang, Z. Hu, J. Gao, and L. Wang, "Learning to Navigate for Fine-Grained Classification," in *Proc. of the ECCV*, 2018, pp. 438–454. [7](#)

- [47] C. Yeh, H. Chen, S. Tsai, and S. Wang, "Disrupting image-translation-based deepfake algorithms with adversarial attacks," in *Proc. of the WACV Workshops*, 2020, pp. 53–62. [3](#), [9](#), [10](#)
- [48] N. Yu, L. S. Davis, and M. Fritz, "Attributing fake images to gans: Learning and analyzing gan fingerprints," in *Proc. of the ICCV*, 2019, pp. 7556–7566. [2](#), [4](#), [9](#), [13](#)
- [49] N. Yu, V. Skripniuk, S. Abdelnabi, and M. Fritz, "Artificial fingerprinting for generative models: Rooting deepfake attribution in training data," *CoRR*, vol. abs/2007.08457, 2020. [2](#), [9](#), [13](#)
- [50] N. Yu, V. Skripniuk, D. Chen, L. Davis, and M. Fritz, "Responsible disclosure of generative models using scalable fingerprinting," *CoRR*, vol. abs/2012.08726, 2020. [2](#), [9](#), [13](#)
- [51] F. Zhang, M. Li, G. Zhai, and Y. Liu, "Multi-branch and Multi-scale Attention Learning for Fine-Grained Visual Categorization," in *Proc. of the MMM*, 2021, pp. 136–147. [7](#)
- [52] J. Zhang, Z. Gu, J. Jang, H. Wu, M. P. Stoecklin, H. Huang, and I. Molloy, "Protecting intellectual property of deep neural networks with watermarking," in *Proc. of the AsiaCCS*, 2018, pp. 159–172. [1](#), [2](#), [12](#)



# Appendices

## A. DETECTION DETAILS

We give a detailed introduction of our detection method. The Negative Log Likelihood (NLL) loss function is used to classify the input samples. As for the holistic regularization in the loss function, it can solve the misleading features who have large values, which means it can help the backbone model treat every feature more fairly when computing the  $x$ . It is a state-of-the-art one class detection method, and we only need positive samples, i.e., clean images, to train the detection model. On the other hand, the adversary do not have verification samples. So, we can only use one class detection method to train a detector. During the training process, the adversary input the differences between clean inputs and their outputs to the detecting model to train it. In the detecting process, the adversary receives the images without knowing whether they are clean images or verification images. Then the adversary inputs the difference between GAN's outputs and inputs. The detecting model gives the label of each one. The adversary applies defense depending on the label from detecting model adaptively. Specifically, the backbone model is ResNet34, which is a common lightweight and powerful deep learning model in computer vision.

## B. FROM PRIVATE TO PUBLIC VERIFIABILITY

As described previously, the algorithm **Verify** only allows verification by honest parties in a private way. This is evolved from the fact that the key  $mk$  will be known once **Verify** is run, which allows the adversary to retrain the model on the verification sample set. It is not a problem for the applications such as intellectual property protection, because there are trusted third parties in the form of judges. However, for practicality, we still hope to design a publicly verifiable method without limiting the number of repeated verifications. To achieve this, we first introduce some additional variables, and then use a powerful cryptographic primitive called the *zero-knowledge proof argument* [10], to convert our fingerprinting scheme from private verifiability to public verifiability. Specifically, we introduce a vector  $\mathbf{e} \in \{0, 1\}^l$ , where  $\mathbf{e}|_0 = \{i \in [l] | \mathbf{e}[i] = 0\}$  and define  $\mathbf{e}|_1$  accordingly. Given such a vector  $\mathbf{e}$ , a verification key  $vk = \{c_v^{(i)}, c_L^{(i)}\}_{i \in [l]}$  can be split into

$$vk|_0^{\mathbf{e}} = \{c_v^{(i)}, c_L^{(i)}\}_{i \in \mathbf{e}|_0} \quad \text{and} \quad vk|_1^{\mathbf{e}} = \{c_v^{(i)}, c_L^{(i)}\}_{i \in \mathbf{e}|_1}$$

Similarly, given the marking key  $mk = (\mathcal{V}, \{h_v^{(i)}, h_L^{(i)}\}_{i \in [l]})$  with  $\mathcal{V} = (v^{(i)}, v_L^{(i)})$  we define

$$mk|_0^{\mathbf{e}} = (\mathcal{V}|_0^{\mathbf{e}}, \{h_v^{(i)}, h_L^{(i)}\}_{i \in \mathbf{e}|_0}) \quad \text{with} \quad \mathcal{V}|_0^{\mathbf{e}} = \{v^{(i)}, v_L^{(i)}\}_{i \in \mathbf{e}|_0}.$$

$mk|_0^{\mathbf{e}}$  is defined accordingly. Further, we assume that there is such a hash function  $H : \{0, 1\}^{p(n)} \rightarrow \{0, 1\}^n$

### A. Zero-Knowledge Arguments

The zero-knowledge argument is a technique that enables a prover  $\mathcal{PR}$  to convince the verifier  $\mathcal{VR}$  that a public statement is true without revealing more information. This core idea can be used to realize the public verifiability of fingerprints in this paper. Specifically, Let TM be the abbreviation of Turing

machine, and iTM means an interactive TM, i.e., a Turing machine with a special communication tape. We define an NP language  $L_R \subseteq \{0, 1\}^*$ , where  $R$  is its related NP-relation, i.e., given a statement  $x$  and a witness  $w$ , if  $x \in L_R$ , then  $(x, w) \in R$  and the TM exploited to define  $L_R$  outputs 1. We write  $R_x = \{w | (x, w) \in R\}$  for the set of witness for a fixed  $x$ . Let  $\mathcal{PR}$  and  $\mathcal{VR}$  be a pair of PPT iTMs. For  $(x, w) \in R$ ,  $\mathcal{PR}$  gets  $w$  as input while  $\mathcal{VR}$  gets an auxiliary random string  $z \in \{0, 1\}^*$ , where  $x$  is the input of both  $\mathcal{PR}$  and  $\mathcal{VR}$ . We use  $\mathcal{VR}^{\mathcal{PR}(a)}(b)$  as the output of the iTM  $\mathcal{VR}$  given an input  $b$  when communicating with an instance of  $\mathcal{PR}$  with input  $a$ .

For language  $L$ , we say that  $(\mathcal{PR}, \mathcal{VR})$  is an interactive zero-knowledge proof system if the following conditions hold: **Correctness.** For any  $x \in L_R$ , there exists a string  $w$  for every  $z$ , such that  $\Pr[\mathcal{VR}^{\mathcal{PR}(x,w)}(x, z) = 1]$  is close to 1 with an overwhelming probability.

**Soundness.** For any  $x \notin L_R$ ,  $\Pr[\mathcal{VR}^{\mathcal{PR}(x,w)}(x, z) = 1]$  is negligible for every PPT iTM  $\mathcal{PR}^*$  and string  $w, z$ .

We say that an interactive system is computationally zero-knowledge for any  $x \in L_R$ , if there is a PPT simulator  $\mathcal{S}$  that satisfies the following condition for any PPT  $\hat{\mathcal{VR}}$ .

$$\{\hat{\mathcal{VR}}^{\mathcal{PR}(x,w)}(x, z)\}_{w \in R_x, z \in \{0, 1\}^*} \approx_c \{\mathcal{S}(x, z)\}_{z \in \{0, 1\}^*}$$

This means that we can obtain all the information by observing the protocol transcript from running a polynomial-time simulator  $\mathcal{S}$ , and the simulator does not know the witness  $w$ .

### B. Technical Intuition

An intuitive way to build a publicly verifiable algorithm **PVerify** is to use a zero-knowledge argument system, where the previously described algorithm **Verify**( $\mathbf{mk}, \mathbf{vk}, \mathbf{M}$ ) is converted to a NP relation  $R$ . Unfortunately, such operations must fail due to Step 1 of **Verify**: testing whether the fingerprint  $\mathcal{V}$  is included in  $mk$  is actually the fingerprint defined above. Therefore, in the interactive demonstration system, we need to access the ground-truth function  $f$ . This requires human help first, but more importantly, it is only possible by exposing fingerprint elements.

In the following, we will give a different solution from the previous one, which requires an additional proof embedded in  $vk$ . This proof is used to show that it is an overwhelming probability that most elements in the verification key do indeed constitute a fingerprint. On this basis, we will design a different verification procedure based on the zero-knowledge system.

### C. A Convincing Argument

If any random part of the elements released by the verification sample set is verified, it implies that most of the elements in the verification sample set are labeled wrongly, which constitute a fingerprint. To solve the problem of proof of misclassification, the cutting and selection technique is exploited. In this technique, the verifier  $\mathcal{VR}$  will ask the prover  $\mathcal{PR}$  to open a random subset of the committed inputs and labels in the verification key. Intuitively, if  $\mathcal{PR}$  makes a commitment for a large number of elements with correct labels (according to  $\mathcal{O}^f$ ), then at least one of them intersects with the subset selected by  $\mathcal{VR}$  with an overwhelming probability, where this subset will be opened by  $\mathcal{PR}$  during the verification

process. Hence, most of the remaining unopened commitments form a correct fingerprint.

To use the cutting and selection technique, the size of the fingerprint must contain  $l > n$  elements. In this paper, we use  $l = 4n$ . Then, we build a protocol between  $\mathcal{PR}$  and  $\mathcal{VR}$  as described below:

**CnC**( $l$ ):

1.  $\mathcal{PR}$  obtains a set of fingerprints with size  $l$  by running  $(mk, vk) \leftarrow \text{KeyGen}(l)$ . Then,  $vk$  is sent to  $\mathcal{VR}$ . We define  $mk = (\mathcal{V}, \{h_v^{(i)}, h_L^{(i)}\}_{i \in [l]}, vk = \{c_v^{(i)}, c_L^{(i)}\}_{i \in [l]}$ .
2.  $\mathcal{VR}$  randomly selects a vector  $\mathbf{e} \leftarrow \{0, 1\}^l$  and sends it to  $\mathcal{PR}$ .
3.  $\mathcal{PR}$  sends  $mk|_1^{\mathbf{e}}$  to  $\mathcal{VR}$ .
4.  $\mathcal{VR}$  checks that for  $i \in \mathbf{e}|_1$  that
  - a.  $\text{Open}(c_v^{(i)}, v^{(i)}, h_v^{(i)}) = 1$ .
  - b.  $\text{Open}(c_L^{(i)}, v_L^{(i)}, h_L^{(i)}) = 1$ , and
  - c.  $v_L^{(i)} \neq f(G(v^{(i)}))$ .

If  $\mathcal{PR}$  chooses exactly one element of the fingerprint in  $vk$  wrongly, this will be revealed to the honest  $\mathcal{VR}$  by the algorithm **CnC**( $l$ ) with a probability of  $1/2$ . In general, a cheating  $\mathcal{PR}$  can add up to  $n$  non-fingerprint elements to the vector  $\mathbf{e}|_0$ . Therefore, if the above verification is passed, there are at least  $n$  correct fingerprint elements in  $vk|_0^{\mathbf{e}}$  with an overwhelming probability.

The above protocol can also be made non-interactive using the Fiat-Shamir transform [1]. Specifically,  $\mathcal{PR}$  can generate the vector  $\mathbf{e}$  by itself through the cryptographic hash function  $H$  to hash the verification key  $vk$ . This makes  $\mathbf{e}$  generated as if it were generated by the honest  $\mathcal{PR}$ , while it is sufficiently random by the guarantees of the hash function to allow the same analysis for cutting and selection.  $\mathcal{PR}$  can recalculate  $\mathbf{e}$  if it is obtained from the hash of  $vk$ , which also means that  $\mathbf{e}$  is generated after  $vk$  is constructed. Based on this, we can transform the above protocol from an interactive one to a non-interactive one with a new algorithm **PkeyGen**:

**PkeyGen**( $l$ ):

1. Run  $(mk, vk) \leftarrow \text{KeyGen}(l)$
2. Compute  $\mathbf{e} \leftarrow H(vk)$ .
3. Set  $mk_p \leftarrow (mk, \mathbf{e})$ ,  $vk_p \leftarrow (vk, mk|_1^{\mathbf{e}})$  and return  $(mk_p, vk_p)$ .

#### D. Concrete Public Verification Algorithm

Different from the previous private verification scheme, the algorithm **Mark** only uses the private subset  $mk|_0^{\mathbf{e}}$  in  $mk_p$  during the publicly verifiable process, and the other parts remain unchanged. Therefore, a publicly verifiable solution follows the following structure: (i)  $\mathcal{VR}$  recalculates the challenger  $\mathbf{e}$ ; (ii)  $\mathcal{VR}$  verifies  $vk_p$  to ensure that all the elements in  $vk|_1^{\mathbf{e}}$  form a valid fingerprint; (iii)  $\mathcal{PR}$  and  $\mathcal{VR}$  run the algorithm **Classify** on  $mk|_0^{\mathbf{e}}$  using an interactive zero-knowledge argument system, and further test whether the conditions for fingerprints are held on  $M$ ,  $mk|_0^{\mathbf{e}}$  and  $vk|_0^{\mathbf{e}}$ .

For any model  $M$ , one can rewrite steps 1 and 3 of the algorithm **Verify** (utilizing  $M$ , **Open**, **Classify**) into a binary circuit  $\mathbf{C}$ .  $\mathbf{C}$  outputs 1 if the prover inputs  $mk|_0^{\mathbf{e}}$  which can open  $vk|_0^{\mathbf{e}}$  correctly and there are enough of these

openings to satisfy the algorithm **Classify**. Both  $\mathcal{PR}$  and  $\mathcal{VR}$  can generate such a circuit  $\mathbf{C}$  and its construction does not involve private information. In the interactive zero-knowledge proof system, we define the relation  $R$  as a Boolean circuit which outputs 1 where  $x = \mathbf{C}$ ,  $w = mk|_0^{\mathbf{e}}$  in the following protocol **PVerify**. **PVerify** will obtain  $M$ ,  $mk_p = (mk, \mathbf{e})$  and  $vk_p = (vk, mk|_1^{\mathbf{e}})$ , where  $vk = \{c_v^{(i)}, c_L^{(i)}\}_{i \in [l]}$ ,  $mk = (\mathcal{V}, \{h_v^{(i)}, h_L^{(i)}\}_{i \in [l]}$ , and  $\mathcal{V} = (v^{(i)}, v_L^{(i)})$  as inputs.

1.  $\mathcal{VR}$  computes  $\mathbf{e}' \leftarrow H(vk)$ . If  $\mathbf{e}'$  does not match  $mk|_1^{\mathbf{e}'}$  in  $vk_p$ , abort. Otherwise, continue assuming  $\mathbf{e} = \mathbf{e}'$ .
2.  $\mathcal{VR}$  checks that for  $i \in \mathbf{e}|_1$  that
  - a.  $\text{Open}(c_v^{(i)}, v^{(i)}, h_v^{(i)}) = 1$ .
  - b.  $\text{Open}(c_L^{(i)}, v_L^{(i)}, h_L^{(i)}) = 1$ .
  - c.  $v_L^{(i)} \neq f(G(v^{(i)}))$ .
 If one of the checks fails, then  $\mathcal{VR}$  aborts.
3.  $\mathcal{PR}$  and  $\mathcal{VR}$  compute a circuit  $\mathbf{C}$  with input  $mk|_0^{\mathbf{e}}$  that outputs 1 if for all  $i \in \mathbf{e}|_0$ :
  - a.  $\text{Open}(c_v^{(i)}, v^{(i)}, h_v^{(i)}) = 1$ .
  - b.  $\text{Open}(c_L^{(i)}, v_L^{(i)}, h_L^{(i)}) = 1$ . $\mathcal{PR}$  and  $\mathcal{VR}$  also need to test that  $\text{Classify}(v^{(i)}, M) = v_L^{(i)}$  for all but  $\epsilon|\mathbf{e}|_0$  elements.
4. Given the relationship  $R$ ,  $\mathcal{PR}$  and  $\mathcal{VR}$  run a zero-knowledge argument using  $\mathbf{C}$  as a statement, where  $\mathcal{PR}$ 's secret input is  $mk|_0^{\mathbf{e}}$  is the witness, and  $\mathcal{VR}$  accepts if the argument is successful.

#### C. VERIFICATION SAMPLES OF DIFFERENT SCHEMES

In this section, we show the verification samples of AE-I, AE-D and CFP-\* in Fig. 1, Fig. 2 and Fig. 3, respectively. For AE-I, it is clear that all GANs can generate high quality outputs from the verification samples, and they are similar visually. However, AE-D does not have the same performance on AttGAN and STGAN as on StarGAN. Because AttGAN and STGAN have more stable generation structures, which means generating disrupted images by them are more difficult. On the other hand, AE-D still achieve a very high SSIM on AttGAN and STGAN, which is shown in Section VII-B, indicating it is not a stable and general fingerprinting scheme.

#### D. HIGH-RESOLUTION FACIAL IMAGES OF CFP-iBDv2

In our experiments, we evaluate the performance of our proposed method by verifying whether the generated fingerprints satisfy the *functionality-preserving*, *unremovability*, and *stealthiness* properties. Here, we present the high-resolution of GAN outputs of CFP-iBDv2 in suffering various degradation, including model compression and corruptions with common image transformations.

##### A. Verification Samples after Different GANs

In Fig. 4, we show our CFP-iBDv2 verification samples' outputs for different GANs. The columns from (e) to (j) indicate the output images from different models manipulated on both clean samples and verification samples. The verification samples do not decrease other GANs outputs' quality in most cases. The outputs of verification samples look similar to outputs of clean samples. It means our CFP-iBDv2 has good functionality-preserving property.

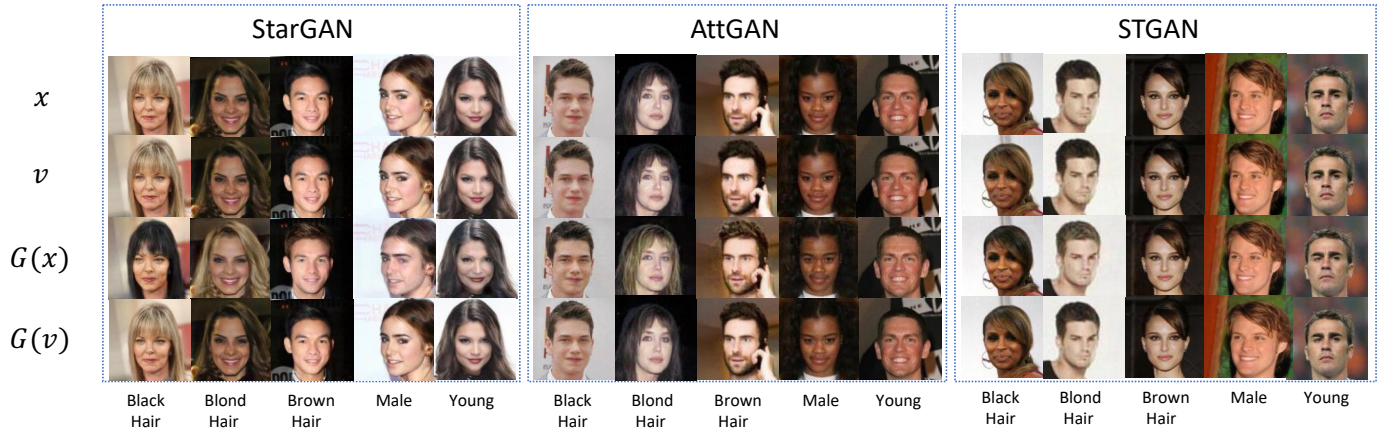


Fig. 1: Fingerprint visualization generated from AE-I for three GAN models with five edited attributes. (a) Clean sample  $x$ ; (b) Verification sample  $v$ ; (c) GAN output of clean sample  $G(x)$ ; (d) GAN output of verification sample  $G(v)$ .

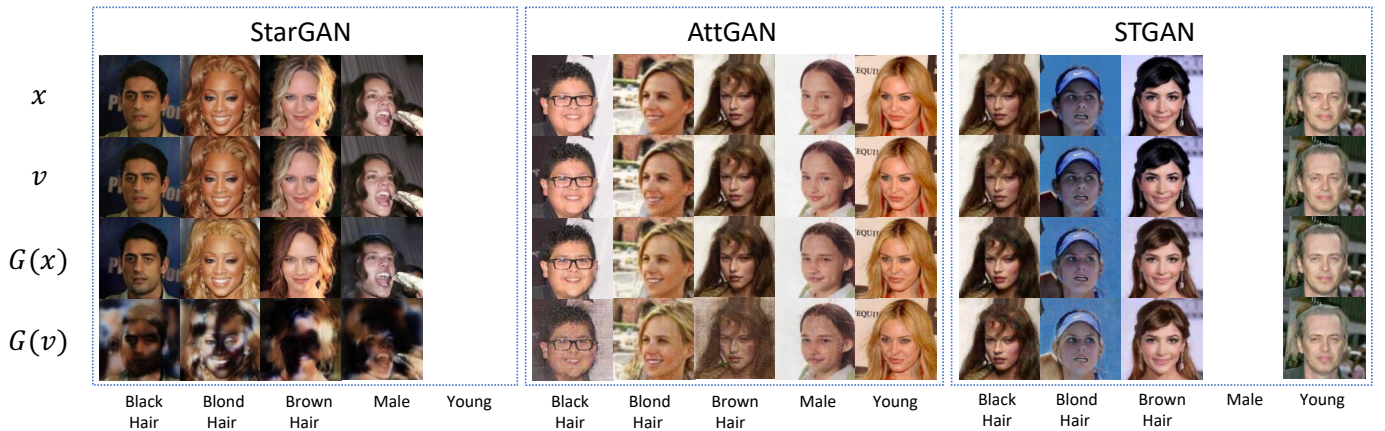


Fig. 2: Fingerprint visualization generated from AE-D for three GAN models with five edited attributes. (a) Clean sample  $x$ ; (b) Verification sample  $v$ ; (c) GAN output of clean sample  $G(x)$ ; (d) GAN output of verification sample  $G(v)$ . Because there are no verification samples for some attributes, we leave these columns blank.

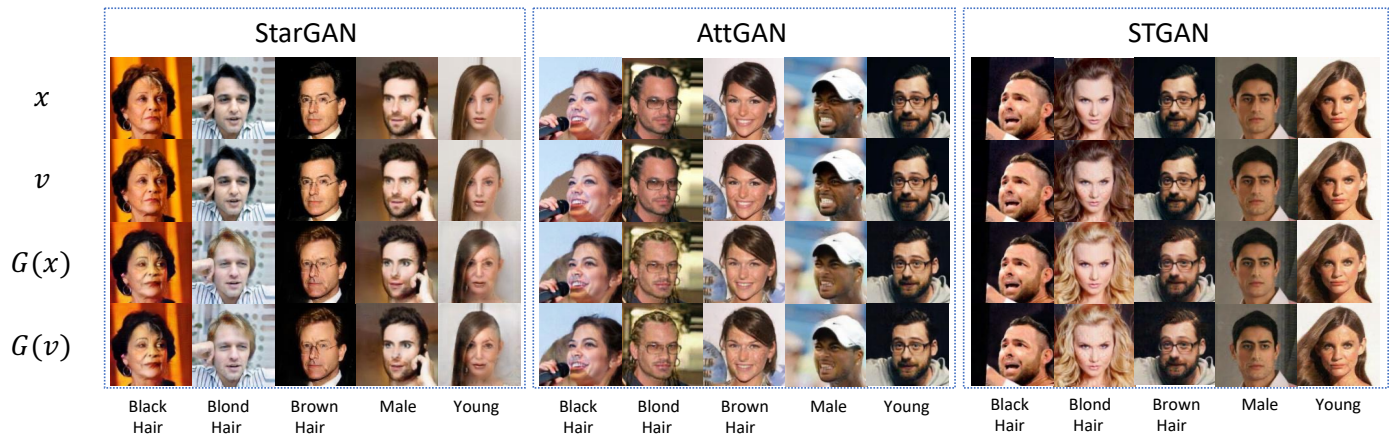


Fig. 3: Fingerprint visualization  $CFP-*$  for three GAN models with five edited attributes. (a) Clean sample  $x$ ; (b) Verification sample  $v$ ; (c) GAN output of clean sample  $G(x)$ ; (d) GAN output of verification sample  $G(v)$ .

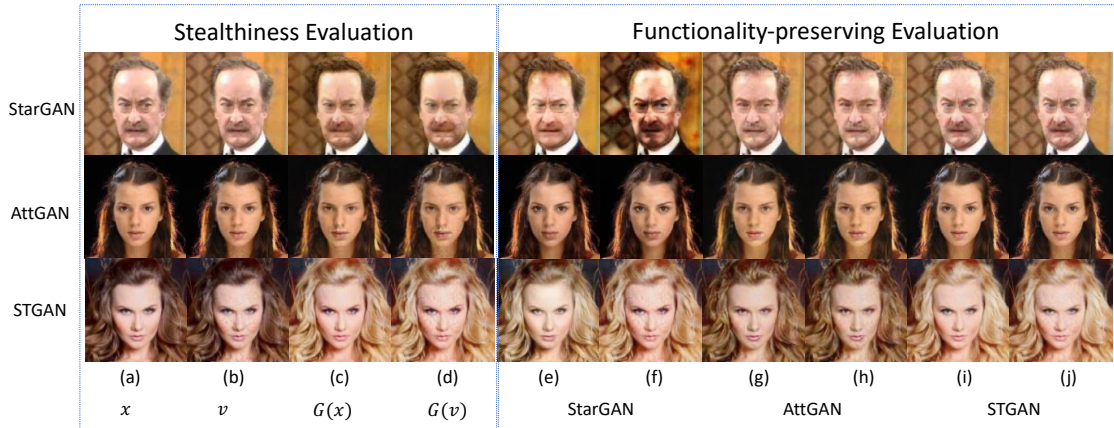


Fig. 4: Manipulated images from StarGAN, AttGAN, and STGAN. The column (e) edits attribute on  $x$  with StarGAN, the column (f) edits attribute on  $v$  with StarGAN, the column (g) edits attribute on  $x$  with AttGAN, the column (h) edits attribute on  $v$  with AttGAN, the column (i) edits attribute on  $x$  with STGAN, the column (j) edits attribute on  $v$  with STGAN.

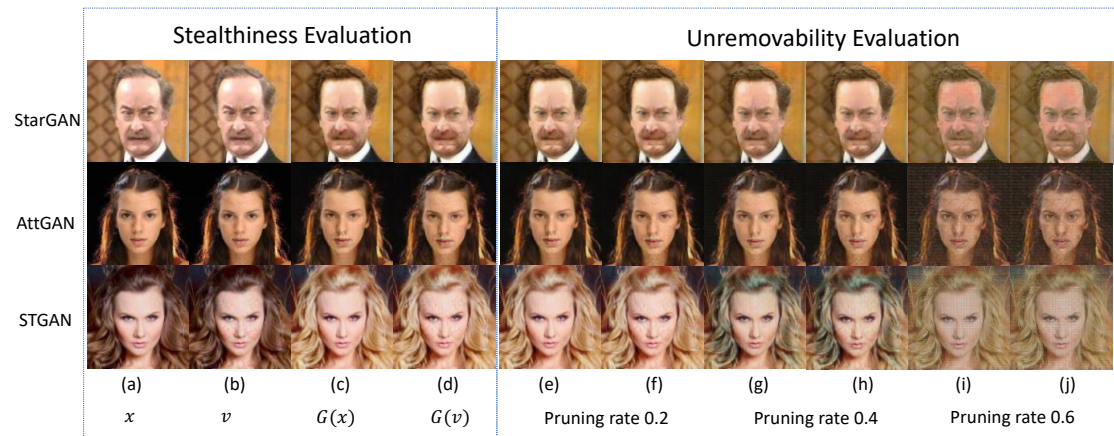


Fig. 5: Images manipulated by StarGAN, AttGAN and STGAN. The column (e) edits attributes on  $x$  with pruning rate 0.2, the column (f) edits attributes on  $v$  with pruning rate 0.2, the column (g) edits attributes on  $x$  with pruning rate 0.4, the column (h) edits attributes on  $v$  with pruning rate 0.4, the column (i) edits attributes on  $x$  with pruning rate 0.6, the column (j) edits attributes on  $v$  with pruning rate 0.6.

### B. Verification Samples suffer Degradation

In evaluating the unremovability of our proposed method, we mainly consider the two different degradation, model transformations and common image transformations. Here, we will give more results under different degrees of degradation.

**Model Transformations.** In evaluating the unremovability against model compression (i.e., pruning), we explore the effectiveness of our method when the GAN model is compressed in various levels. In Fig. 5, the column (e) to (h) indicate the manipulated images with compressed models when the pruning rate is not larger than 0.4. We can find that the GAN’s outputs maintain a high-quality visualization, thus the pruning rate no more than 0.4 is an appropriate setting in our experiment. Furthermore, if the pruning rate is higher, when it is 0.6, the outputs is not satisfying for a user. We further compare more experimental results under various pruning rates showing in the Fig. 6. When the pruning rate is smaller than 0.5, the MSV

(%) is high enough to pass the verification (the threshold is 0.8). With the pruning rate increasing, the MSV (%) will drop slowly at first and decrease significantly after the pruning rate is higher than 0.5. Because the outputs’ quality is not good enough for the backdoor classifier to recognize the triggers.

**Image Transformations.** The GAN’s outputs will always be corrupted by various image transformations when spreading in the social models. Fig. 7 presents the visualization of GAN’s outputs by employing four different types of common image transformations, including adding *Gaussian noises*, *blurring*, *JPEG compression*, and *centering cropping*. Here, the parameters of these transformations are described in Section VII-D. In Fig. 8, we show the MSV (%) under different transformation magnitudes, which transformation applies on the outputs of the GAN. Clearly, our CFP-iBDv2 is robust under blurring and compression. These two transformations have trivial influence during the verification process. As for adding Gaussian noise, CFP-iBDv2 is robust on the AttGAN, and when the noise

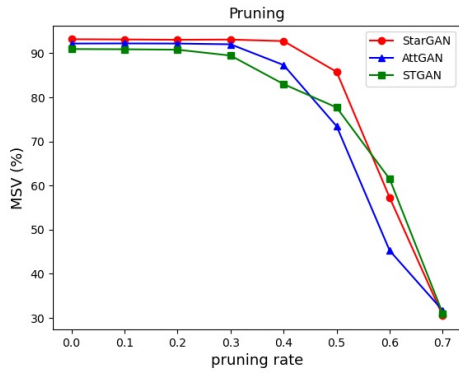


Fig. 6: MSV (%) of CFP-iBDv2 under different pruning rates.

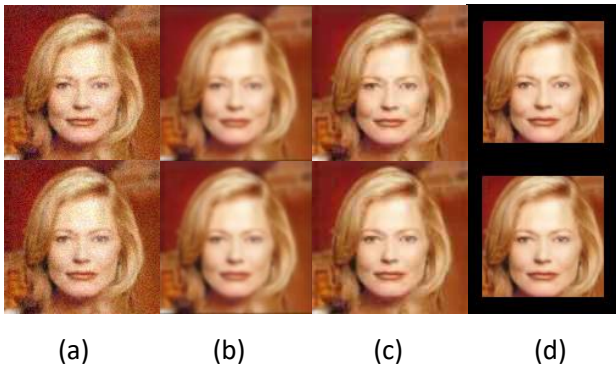


Fig. 7: Visualization of GAN output images corrupted by four types of image transformations. The first row is GAN outputs from clean images. The second row is GAN outputs from verification samples. (a) adding Gaussian Noise, (b) blurring, (c) JPEG compression, (d) centering cropping.

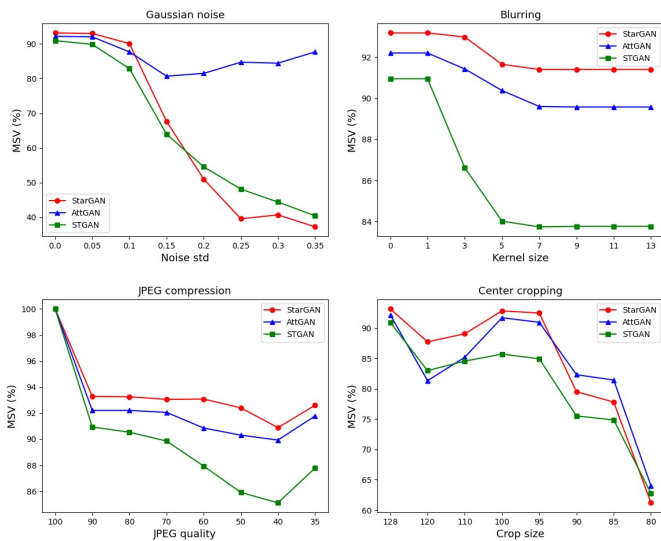


Fig. 8: MSV (%) of CFP-iBDv2 under different settings of transformations, which are applied on the outputs of the GAN.

std is higher than 0.1, the verification process will fail on the StarGAN and STGAN. Center cropping can significantly decline the completeness of backdoor triggers, resulting in the verification failure. Our CFP-iBDv2 can still work when the cropping size is bigger than 90, which is an excellent result.

After the comprehensive experiments on model pruning and image transformations, our CFP-iBDv2 shows impressive *functionality-preserving*, *unremovability*, and *stealthiness*. It can defend against gentle and medium image modification and model compression. More than that, its outputs are visually indistinguishable for humans.